

Conformation, Solutions, and Molecular Weight

Solvents are frequently used during the polymerization process (Chapter 2), during fabrication (e.g., film casting, fiber formation, and coatings), and for determining molecular weights and molecular-weight distributions. Interactions between a polymer and solvent influence chain dimensions (i.e., conformations) and, more importantly, determine solvent activities. The measurement of osmotic pressure and scattered-light intensity from dilute polymer solutions—techniques based upon the principles of polymer-solution thermodynamics—are the primary methods used to determine number-average and weight-average molecular weights, respectively. Other solution-property techniques, such as the determination of intrinsic viscosity and gel-permeation chromatography (GPC), are widely used as rapid and convenient methods to determine polymer molecular weight and, in the case of GPC, molecular-weight distributions as described in this chapter.

3.1 POLYMER CONFORMATION AND CHAIN DIMENSIONS

As briefly discussed in Chapter 1, the *configuration* of a polymer chain refers to the stereochemical arrangement of atoms along that chain. Examples include tactic and geometric isomers, which are determined by the mechanism of the polymerization and, therefore, cannot be altered without breaking primary valence bonds. In contrast, polymer chains in solution are free to rotate around individual bonds, and almost a limitless number of *conformations* or chain orientations in three-dimensional space are possible for long, flexible macromolecules.

To describe the conformation of polymer molecules, a highly idealized model of a *random flight* or *freely jointed* and *volumeless* chain is often used as a starting point. Such a hypothetical chain is assigned n freely jointed links having equal length, ℓ . If one end of this hypothetical chain is fixed at the origin of a Cartesian coordinate system, the other end of the chain has some finite probability of being at any other coordinate position, as illustrated by Figure 3-1. One of the many possible conformations, and the simplest, for this idealized chain is the fully extended (i.e., linear) chain where the end-to-end distance, r , is simply

$$r = n\ell. \quad (3.1)$$

Flory [1] was the first to derive an expression for the probability of finding one end of the freely jointed polymer chain in some infinitesimal volume ($dV = dx \cdot dy \cdot dz$) around a particular coordinate point (x, y, z) when one end of the chain is fixed at the origin of a Cartesian coordinate system, as illustrated in Figure 3-1. The probability is given by a *Gaussian distribution* in the form

$$\omega(x, y, z) dx dy dz = \left(\frac{b}{\pi^{1/2}} \right)^3 \exp(-b^2 r^2) dx dy dz \quad (3.2)$$

where $\omega(x, y, z)$ is called the Gaussian distribution function, r is the radius of a spherical shell centered at the origin where

$$r^2 = x^2 + y^2 + z^2, \quad (3.3)$$

and

$$b^2 = \frac{3}{2nl^2}. \quad (3.4)$$

Alternatively, the probability that a chain displacement length has a value in the range r to $r+dr$ is given as

$$\omega(r)dr = \left(\frac{b}{\pi^{1/2}}\right)^3 \exp(-b^2 r^2) 4\pi r^2 dr \quad (3.5)$$

where $\omega(r)$ is called the *radial* distribution function. The radial distribution function for a freely jointed polymer chain consisting of 10^4 freely jointed links each of length 2.5 \AA is plotted as a function of the radial distance, r , in Figure 3-2.

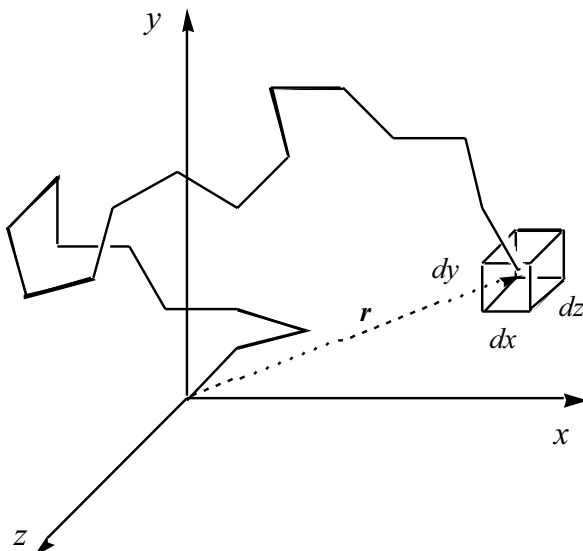


Figure 3-1 Illustration of a random conformation of an idealized freely jointed polymer chain having 20 segments of equal length. The end-to-end distance of this conformation is indicated as r . With one end of the chain fixed at the origin of the Cartesian coordinate system, the probability of finding the other end in some infinitesimal volume element ($dV = dx \cdot dy \cdot dz$) is given by the Gaussian distribution function (eq (3.2)).

The mean-square end-to-end distance is obtained from the second moment of the radial distribution function as

$$\langle r^2 \rangle = \frac{\int_0^\infty r^2 \omega(r) dr}{\int_0^\infty \omega(r) dr}. \quad (3.6)$$

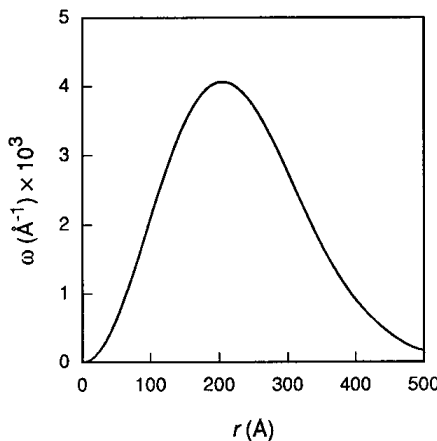


Figure 3-2 The radial distribution function calculated (eq. (3.5)) for a hypothetical polymer chain consisting of 10^4 freely jointed segments of length 2.5 Å.

Substitution of the radial-distribution function (eq. (3.5)) into eq. (3.6) and evaluating the integral gives the mean-square end-to-end distance of the freely jointed and volumeless chain as

$$\langle r^2 \rangle = n\ell^2. \quad (3.7)$$

Alternatively, the root-mean-square end-to-end distance, $\langle r^2 \rangle^{1/2}$, of the freely rotating chain is given as

$$\langle r^2 \rangle^{1/2} = n^{1/2}\ell. \quad (3.8)$$

Real polymer chains differ from the above idealized, freely jointed model in the following three significant ways:

- **Valence angles of real bonds are fixed.** For example, the tetrahedrally bonded C–C bond angle is 109.5° . Introducing fixed bond angles results in an expansion of the chain expressed by the mean-square end-to-end distance as (for large n)

$$\langle r^2 \rangle = n\ell \frac{1 - \cos\theta}{1 + \cos\theta} \quad (3.9)$$

where θ is the valence bond angle, as illustrated for an extended chain conformation in Figure 3-3. In the case of tetrahedral valence angles, $\cos \theta \approx -1/3$, and, therefore,

$$\langle r^2 \rangle = 2n\ell^2. \quad (3.10)$$

Comparison of this result with that of eq. (3.7) indicates that restricting the valence angle to 109.5° results in a doubling of the mean-square end-to-end distance compared to the freely rotating model.

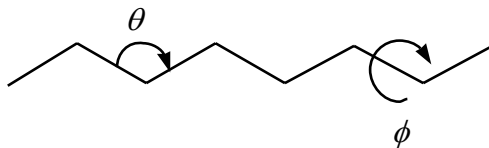


Figure 3-3 Illustration of an extended polymer chain showing the valence bond angle, θ , and bond-rotation angle, ϕ .

- **Rotations of polymer chains may be hindered due to steric interference from bulky substituent groups.** As illustrated by the potential-energy diagram shown in Figure 3-4, overlap of bulky substituent groups on adjacent carbon atoms results in a high-energy, unfavorable conformational state. The result of this steric interference is to further expand chain dimensions over the random-flight model. Equation (3.7) may be further modified to include the effects of both fixed bond angles and hindered rotations as

$$\langle r^2 \rangle = n\ell \frac{1 - \cos \theta}{1 + \cos \theta} \frac{1 + \langle \cos \phi \rangle}{1 - \langle \cos \phi \rangle} \quad (3.11)$$

where $\langle \cos \phi \rangle$ represents the average cosine of the bond-rotation angle, ϕ , identified in Figure 3-3. This second contribution is much more difficult to evaluate but can be obtained by statistical-weighting methods, as discussed by Flory [2].

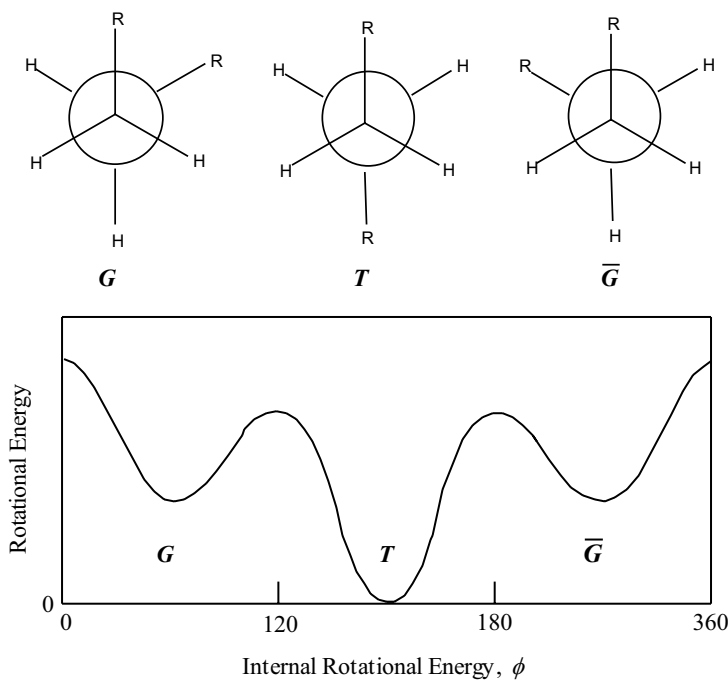


Figure 3-4 Newman projections (top) of three lowest energy projections of two adjacent bond atoms with substituent group R. In the case of a polymer chain, R represents all chain segments before and after the bond in question. The potential-energy diagram (bottom) displays the three lowest energy rotational states—*trans* (*T*) and the two *gauche* forms, *G* and \bar{G} .

- **Real chain bonds have a finite (van der Waals) volume and, therefore, some volume is excluded.** This means that a real bond cannot occupy the same space of any other bond—a condition not imposed in the random-flight model. As in the case of restricted rotation, the effect of excluded volume is to increase the spatial dimensions of the polymer chain over those of the random-flight model.

Beyond the calculation of mean-square end-to-end distances, the conformations of realistic polymer models can be simulated by computer. For example, Figure 3-5 shows the results of a Monte Carlo simulation of the conformation of a small polyethylene chain having 200 skeletal bonds using values of actual bond lengths, bond angles, and the known preference for *trans*-rotational states for this polymer [3].

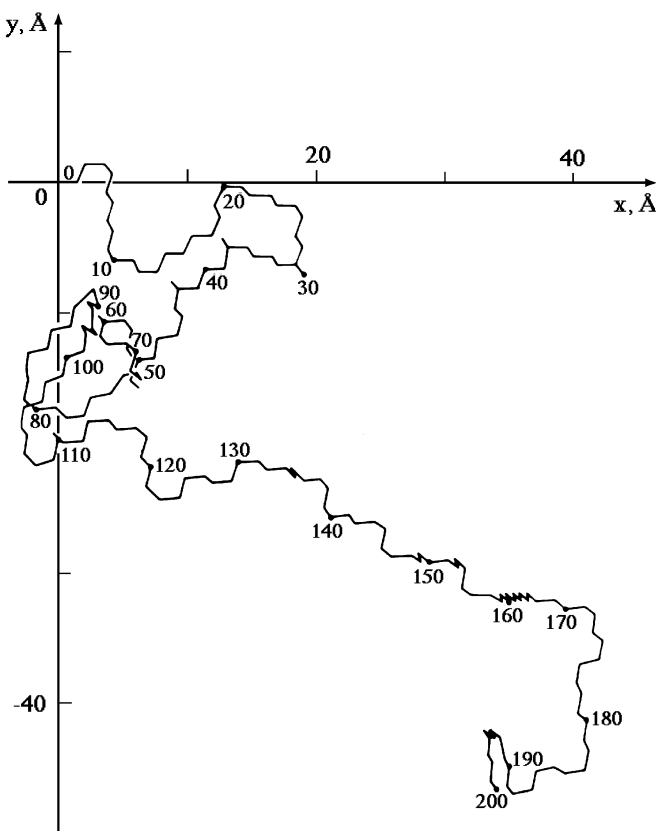


Figure 3-5 A three-dimensional computer simulation of a conformation of a small polyethylene chain (200 bonds) projected on the plane of the graph. Used with permission from the Journal of Chemical Education, 1981. **58**(11): p. 898–903. Copyright © 1981, Division of Chemical Education, Inc.

As a convenient way to express the size of a real polymer chain in terms of parameters that can be readily measured, the freely rotating chain model (eq. (3.7)) may be modified to include the effects of fixed bond angles, restricted rotation, and excluded volume on the root-mean-square end-to-end distance in the following way:

$$\langle r^2 \rangle^{1/2} = \alpha(nC_\infty)^{1/2} \ell. \quad (3.12)$$

In this expression, α is called the *chain expansion factor*, which is a measure of the effect of excluded volume, and C_∞ is called the *characteristic ratio*, which contains the contributions from both fixed valence angles and restricted chain rotations. For large polymer chains, typical values of C_∞ range from about 5 to 10 as shown by some representative values in Table 3-1. Another way to represent eq. (3.12) is by use of an *unperturbed* root-mean-square end-to-end distance, $\langle r^2 \rangle_o^{1/2}$, as

$$\langle r^2 \rangle^{1/2} = \alpha \langle r^2 \rangle_o^{1/2}. \quad (3.13)$$

Table 3-1 Examples of Characteristic Ratios [4]

Polymer	C_∞
Polyethylene	6.7
Polystyrene	10.
Polypropylene	5.8
Poly(vinyl alcohol)	8.3
Poly(vinyl acetate)	9.4
Poly(vinyl chloride)	7.6
Poly(methyl methacrylate)	8.2
Poly(ethylene oxide)	4.2
Polycarbonate	2.4

Comparison of eqs. (3.12) and (3.13) indicates that *unperturbed* dimensions are those of a real polymer chain in the absence of excluded-volume effects (i.e., for $\alpha = 1$). By equating eqs. (3.12) and (3.13), the characteristic ratio* is obtained as the ratio of the unperturbed mean-square end-to-end distance to the mean-square end-to-end distance of the freely jointed model (eq. (3.7)):

$$C_\infty = \frac{\langle r^2 \rangle_o}{nl^2}. \quad (3.14)$$

Unperturbed dimensions are realized in the case of a polymer in solution with a thermodynamically poor solvent at a temperature near incipient precipitation. This temperature is called the *theta (θ) temperature*. Experiments using small-angle neutron scattering have indicated that the dimensions of polymer chains in the amorphous solid state are also unperturbed [5]. In solution with a good solvent (i.e.,

* The characteristic ratio can be calculated from a knowledge of actual valence angles, θ , and the statistical weighting of torsional angles, ϕ (see eq. (3.11)), as

$$C_\infty = \frac{1 - \cos \theta}{1 + \cos \theta} \frac{1 + \langle \cos \phi \rangle}{1 - \langle \cos \phi \rangle}.$$

$\alpha > 1$), where polymer–solvent interactions are stronger than polymer–polymer or solvent–solvent interactions, dimensions of the polymer chain are expanded over those in the unperturbed state ($\alpha = 1$).

3.2 THERMODYNAMICS OF POLYMER SOLUTIONS

It was recognized in the 1940s that the thermodynamics of polymeric systems needs to be treated in a special way. In 1942, Gee and Treloar [6] reported that even dilute polymer solutions deviated strongly from ideal-solution behavior. In these early experiments, a high-molecular-weight rubber was equilibrated with benzene vapor in a closed system and the partial pressure of the benzene (the solvent), p_1 , was measured. The solvent activity, a_1 , was calculated as the ratio of p_1 to the saturated vapor pressure of pure benzene, p_1^o , at the system temperature as

$$a_1 = \frac{p_1}{p_1^o}. \quad (3.15)$$

Experimental benzene activity is plotted as a function of the *volume fraction* of rubber, ϕ_2 , in Figure 3-6. These data are compared with predictions of *Raoult's law* for an ideal solution given as

$$p_1 = x_1 p_1^o \quad (3.16)$$

where x_1 is the mole fraction of the solvent. Substitution of eq. (3.16) into eq. (3.15) yields the result that $a_1 \equiv x_1$ for an ideal solution. As the experimental data (Figure

* By definition, the activity of the i th component in a mixture is defined as

$$a_i = \frac{\hat{f}_i}{f_i^o}$$

where \hat{f}_i is the fugacity of that component in the mixture and f_i^o is the standard-state fugacity, usually the fugacity of the pure liquid component at the system temperature. In the limit of low pressure at which the vapor mixture becomes ideal, the two fugacities may be replaced by the corresponding pressure terms (i.e., $\hat{f}_i = p_i = x_i p$ and $f_i^o = p_i^o$). If the vapor phase is nonideal, the solvent activity can be obtained from the relationship

$$a_i = \frac{p_i}{p_i^o} \exp\left[-\frac{B}{RT}(p_i^o - p_i)\right]$$

where B is the second virial coefficient of the pure vapor at the system temperature.

3-6) show, polymer-solution behavior follows a strong *negative* deviation from Raoult's ideal-solution law.

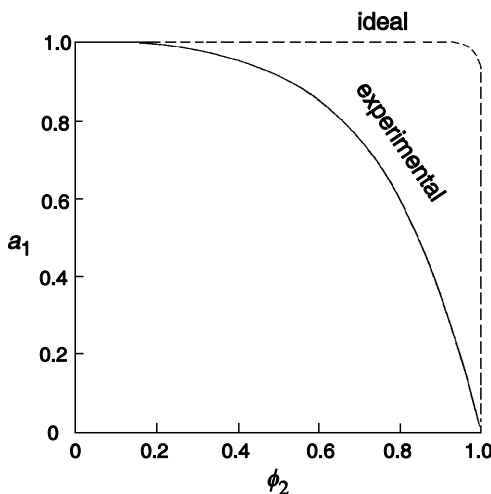


Figure 3-6 Plot of benzene activity, a_1 , versus volume fraction of rubber, ϕ_2 . Dashed line represents ideal-solution behavior. Reprinted from Paul J. Flory, *Principles of Polymer Chemistry*. Fig. 108, p. 496. Copyright © 1953 Cornell University and copyright © 1981 Paul J. Flory. Used by permission of the publisher, Cornell University Press.

3.2.1 The Flory–Huggins Theory

In the early 1940s, Paul Flory [7, 8] and Maurice Huggins [9, 10], working independently, developed a theory based upon a simple lattice model that could be used to understand the nonideal nature of polymer solutions. An excellent review of the development of the lattice model has been given by Flory [11]. In the *Flory–Huggins model*, the lattice sites, or holes, are chosen to be the size of the solvent molecule. As the simplest example, consider the mixing of a low-molecular-weight solvent (component 1) with a low-molecular-weight solute (component 2). The solute molecule is assumed to have the same size as a solvent molecule, and therefore only one solute or one solvent molecule can occupy a single lattice site at a given time. The lattice model for this case is illustrated in Figure 3-7.

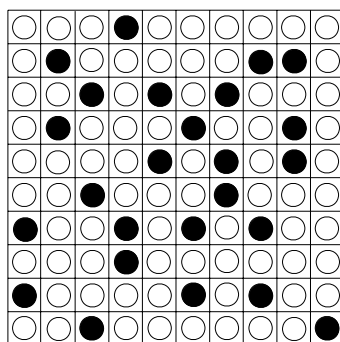


Figure 3-7 Representation of two-dimensional Flory–Huggins lattice containing solvent molecules (\circ) and a low-molecular-weight solute (\bullet).

The increase in entropy due to mixing of a solvent and solute, ΔS_m , may be obtained from the *Boltzmann relation*

$$\Delta S_m = k \ln \Omega \quad (3.17)$$

where k is Boltzmann's constant ($1.38 \times 10^{-23} \text{ J K}^{-1}$) and Ω gives the total number of ways of arranging n_1 indistinguishable solvent molecules and indistinguishable n_2 solute molecules, where $N = n_1 + n_2$ is the total number of lattice sites. The probability function is given as

$$\Omega = \frac{N!}{n_1! n_2!}. \quad (3.18)$$

Using the Stirling approximation

$$\ln n! = n \ln n - n \quad (3.19)$$

leads to the expression for the entropy of mixing *per molecule* as

$$\Delta S_m = -k(n_1 \ln x_1 + n_2 \ln x_2). \quad (3.20)$$

Alternatively, the *molar* entropy of mixing can be written as

$$\boxed{\Delta S_m = -R(x_1 \ln x_1 + x_2 \ln x_2)}$$

(3.21)

where R is the ideal gas constant* and x_1 is the mole fraction of the solvent given as

* $R = N_A k$ where N_A is Avogadro's number.

$$x_1 = \frac{n_1}{n_1 + n_2} . \quad (3.22)$$

Equation (3.21) is the well-known relation for the entropy change due to mixing of an *ideal* mixture, which can also be obtained from classical thermodynamics of an ideal solution following the Lewis–Randall law.* Equation (3.20) can be written for a multicomponent system having N components as

$$\Delta S_m^{\text{id}} = -R \sum_{i=1}^N x_i \ln x_i . \quad (3.23)$$

* The relationship between the partial-molar Gibbs free energy and fugacity is given as

$$d\bar{G}_i \equiv d\mu_i = RT d \ln \hat{f}_i .$$

Integration from the standard state to some arbitrary state gives

$$\bar{G}_i - G_i^\circ \equiv \overline{\Delta G}_i = RT \ln \frac{\hat{f}_i}{f_i^\circ}$$

where \hat{f}_i is the fugacity of component i in a mixture and f_i° is the standard-state fugacity. Substitution of the Lewis–Randall law

$$\hat{f}_i^{\text{id}} = x_i f_i^\circ$$

gives

$$\overline{\Delta G}_i^{\text{id}} = RT \ln x_i .$$

Since the thermodynamic properties of a solution are the sum of the product of the mole fraction and the partial-molar property of each of m components in the mixture, it follows that the molar change in Gibbs free energy of an ideal solution is then expressed as

$$\boxed{\Delta G^{\text{id}} = \sum_{i=1}^m x_i \left(\overline{\Delta G}_i^{\text{id}} \right) = RT \sum_{i=1}^m x_i \ln x_i} .$$

Since

$$\overline{\Delta G}_i^{\text{id}} = \overline{\Delta H}_i^{\text{id}} - T \overline{\Delta S}_i^{\text{id}}$$

and $\overline{\Delta H}_i^{\text{id}} = 0$ for an ideal solution, we have

$$\overline{\Delta S}_i^{\text{id}} = -\frac{1}{T} \overline{\Delta G}_i^{\text{id}} = -R \ln x_i$$

and

$$\boxed{\Delta S^{\text{id}} = \sum_{i=1}^m x_i \left(\overline{\Delta S}_i^{\text{id}} \right) = -R \sum_{i=1}^m x_i \ln x_i} .$$

The entropy of mixing a low-molecular-weight solvent with a *high*-molecular-weight polymer is smaller than given by eq. (3.20) for a low-molecular-weight mixture. This is due to the loss in conformational entropy resulting from the linkage of individual repeating units along a polymer chain compared to the less ordered case of unassociated low-molecular-weight solute molecules dispersed in a low-molecular-weight solvent. In the development of an expression for ΔS_m for a high-molecular-weight polymer in a solvent, the lattice is established by dividing the polymer chain into r segments, each the size of a solvent molecule, where r is the ratio of polymer volume to solvent volume (i.e., a lattice site). For n_2 polymer molecules, the total number of lattice sites is then $N = n_1 + rn_2$. A lattice containing low-molecular-weight solvent molecules and a single polymer chain is illustrated in Figure 3-8.

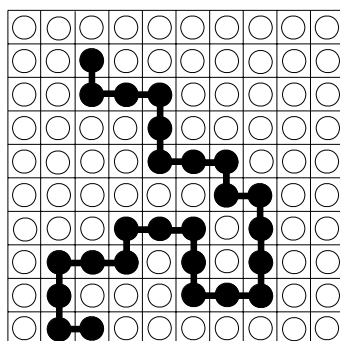


Figure 3-8 Lattice model for a polymer chain in solution. Symbols represent solvent molecules (○) and polymer-chain segments (●).

The expression for the entropy change due to mixing obtained by Flory and Huggins is given as

$$\Delta S_m = -k(n_1 \ln \phi_1 + n_2 \ln \phi_2) \quad (3.24)$$

where ϕ_1 and ϕ_2 are the lattice *volume* fractions of solute (component 1) or polymer (component 2), respectively. These are given as

$$\phi_1 = \frac{n_1}{n_1 + rn_2} \quad (3.25)$$

and

$$\phi_2 = \frac{rn_2}{n_1 + rn_2}. \quad (3.26)$$

For a polydisperse polymer, eq. (3.24) can be modified as

$$\Delta S_m = -k \left(n_1 \ln \phi_1 + \sum_{i=2}^N n_i \ln \phi_i \right) \quad (3.27)$$

where the summation is over all polymer chains (N) in the molecular-weight distribution. For simplicity, the most commonly used form of the entropy expression, eq. (3.24), will be used in further discussion. Equation (3.24) provides the entropy term in the expression for the Gibbs free energy of mixing, ΔG_m , of a polymer solution given as

$$\Delta G_m = \Delta H_m - T\Delta S_m. \quad (3.28)$$

Once an expression for the enthalpy of mixing, ΔH_m , is known, expressions for the chemical potential and activity of the solvent can be obtained as

$$\Delta \mu_1 = \mu_1 - \mu_1^\circ = \overline{\Delta G}_m = \left(\frac{\partial \Delta G_m}{\partial n_1} \right)_{T,p} \quad (3.29)$$

where $\overline{\Delta G}_m$ is the partial-molar Gibbs free energy of mixing and the activity is related to the chemical potential as

$$\ln a_1 = \frac{\Delta \mu_1}{kT}. \quad (3.30)$$

For an *ideal* solution, $\Delta H_m = 0$. Solutions for which $\Delta H_m \neq 0$ but for which ΔS_m is given by eq. (3.20) are termed *regular* solutions and are the subject of most thermodynamic models for polymer mixtures. The expression that Flory and Huggins gave for the enthalpy of mixing is

$$\Delta H_m = z n_1 r_1 \phi_2 \Delta \omega_{12} \quad (3.31)$$

where z is the lattice coordination number or number of cells that are first neighbors to a given cell, r_1 represents the number of “segments” in a solvent molecule for consideration of the most general case, and $\Delta \omega_{12}$ is the change in internal energy for formation of an unlike molecular pair (solvent–polymer or 1–2) contacts given by the *mean-field expression* as

$$\Delta \omega_{12} = \omega_{12} - \frac{1}{2} (\omega_{11} + \omega_{22}) \quad (3.32)$$

where ω_{ij} is the energy of i – j contacts. It is clear from eqs. (3.31) and (3.32) that an ideal solution ($\Delta H_m = 0$) is one for which the energies of 1–1, 1–2, and 2–2 molecular interactions are equal.

Since z and ω_{12} have the character of empirical parameters, it is useful to define a single energy parameter called the Flory *interaction parameter*, χ_{12} , given as

$$\chi_{12} = \frac{zr_1\Delta\omega_{12}}{kT}. \quad (3.33)$$

The interaction parameter is a dimensionless quantity that characterizes the interaction energy per solvent molecule (having r_1 segments) divided by kT . As eq. (3.33) indicates, χ_{12} is inversely related to temperature but is independent of concentration in the Flory–Huggins model.

The expression for the enthalpy of mixing may then be written by combining eqs. (3.31) and (3.33) as

$$\Delta H_m = kT\chi_{12}n_1\phi_2. \quad (3.34)$$

Combining the expression for the entropy (eq. (3.24)) and enthalpy (eq. (3.34)) of mixing gives the well-known Flory–Huggins expression for the Gibbs free energy of mixing

$$\boxed{\Delta G_m = kT(n_1 \ln \phi_1 + n_2 \ln \phi_2 + \chi_{12}n_1\phi_2)}. \quad (3.35)$$

From this relationship, the activity of the solvent (eq. (3.30)) can be obtained from eq. (3.35) as

$$\ln a_1 = \ln(1 - \phi_2) + \left(1 - \frac{1}{r}\right)\phi_2 + \chi_{12}\phi_2^2. \quad (3.36)$$

In the case of high-molecular-weight polymers for which the number of solvent-equivalent segments, r ,^{*} is large, the $1/r$ term within parentheses on the RHS of eq. (3.36) can be neglected to give

$$\boxed{\ln a_1 = \ln(1 - \phi_2) + \phi_2 + \chi_{12}\phi_2^2}. \quad (3.37)$$

The Flory–Huggins equation is still widely used and has been largely successful in describing the thermodynamics of polymer solutions; however, there are a number of important limitations of the original expression that should be emphasized. The most important are the following:

^{*} For a polymer sample containing a distribution of molecular weights, r may be taken to be the number-average degree of polymerization, \bar{X}_n .

- Solutions are sufficiently concentrated that they have uniform segment density.
- There is no volume change of mixing (whereas favorable interactions between polymer and solvent molecules should result in a *negative* volume change).
- There are no energetically preferred arrangements of polymer segments and solvent molecules in the lattice.
- The Flory interaction parameter, χ_{12} , is independent of composition.

There have been a number of subsequent developments to extend the applicability of the original Flory–Huggins theory and to improve agreement between theoretical and experimental results. For example, Flory and Krigbaum [12] have developed a thermodynamic theory for dilute polymer solutions, which was described in Flory's original text [1]. Koningsveld [13] and others have improved the agreement of the original Flory–Huggins theory with experimental data by an empirical modification of χ_{12} to include a composition dependence and to account for polydispersity. Both of these approaches are presented briefly in the following section. More recent approaches employ equation-of-state theories such as those developed by Flory [11] and others for which a volume change of mixing can be incorporated. These are developed later in Section 3.2.3.

3.2.2 Flory–Krigbaum and Modified Flory–Huggins Theories

Flory–Krigbaum Theory. Flory and Krigbaum [12] have provided a model to describe the thermodynamics of a dilute polymer solution. In contrast to the case of a semidilute solution addressed by the Flory–Huggins theory, segmental density can no longer be considered to be uniform. In their development, Flory and Krigbaum viewed the dilute solution as a dispersion of clouds consisting of polymer segments surrounded by regions of pure solvent. For a dilute solution, the expression for solvent activity was given as

$$\ln a_1 = (\kappa_1 - \psi_1) \phi_2^2 \quad (3.38)$$

where κ_1 and ψ_1 are heat and entropy parameters,^{*} respectively. Flory and Krigbaum defined an “ideal” or *theta* (θ) temperature as

* $\overline{\Delta H}_1 = RT\kappa_1\phi_2^2$; $\overline{\Delta S}_1 = R\psi_1\phi_2^2$.

$$\theta = \frac{\kappa_1 T}{\psi_1} \quad (3.39)$$

from which eq. (3.38) can be written as

$$\ln \alpha_1 = -\psi_1 \left(1 - \frac{\theta}{T} \right) \phi_2^2. \quad (3.40)$$

It follows from eq. (3.40) that solvent activity approaches unity as temperature approaches the θ temperature. At the θ temperature, the dimensions of a polymer chain collapse to unperturbed dimensions (i.e., in the absence of excluded-volume effects), as described in Section 3.1.

Modified Flory–Huggins. In the original lattice theory, χ_{12} was given an inverse dependence upon temperature (eq. (3.33)) but there was no provision for a concentration dependence, which experimental studies have shown to be important. Koningsveld [13] and others have introduced an empirical dependence to improve the agreement with experimental data by casting the Flory–Huggins expression in the general form

$$\Delta G_m = RT(\phi_1 \ln \phi_1 + \phi_2 \ln \phi_2 + g\phi_1\phi_2). \quad (3.41)$$

In eq. (3.41), g is an interaction energy term for which the concentration dependence can be given as a power series in ϕ_2 as

$$g = g_0 + g_1\phi_2 + g_2\phi_2^2 + \dots \quad (3.42)$$

where each g term, g_k ($k = 0, 1, 2, \dots$), has a temperature dependence that can be expressed in the form

$$g_k = g_{k,1} + \frac{g_{k,2}}{T}. \quad (3.43)$$

3.2.3 Equation-of-State Theories

Although the Flory–Huggins theory is still useful as a starting point for describing polymer thermodynamics, there are a number of weaknesses. For example, the simple lattice model does not accommodate a volume change of mixing, which can be significant in the case of a thermodynamically good solution. Such an inability to incorporate a volume change of mixing can lead to particular weakness in the prediction of phase equilibrium. Substantial improvement in the theoretical treatment of polymer thermodynamics has been obtained by adopting a statistical-thermodynamics approach based upon an equation of state (EOS) as first proposed by

Flory [14]. Other successful EOS theories have been proposed by Sanchez [15] and by Simha [16]. For the purpose of providing an introduction to the use of EOS theories in the treatment of polymer thermodynamics, only the Flory EOS theory, which was the first and is still widely used, is described in this section.

Flory Equation of State. Thermodynamic variables in statistical thermodynamics are obtained from a suitable partition function, which can be a simple or complex function depending upon the size and physical state of the molecule being considered. The simplest partition functions are obtained for monatomic and diatomic gases such as helium and nitrogen. The partition function chosen by Flory for the polymer was obtained from contributions by internal (i.e., intramolecular chemical-bond forces) and external (i.e., intermolecular forces) degrees of freedom. The internal contribution is dependent upon temperature, while the external contribution is dependent upon both temperature and volume. The Flory partition function can be given in reduced form as [11]

$$Z = Z_{\text{comb}} \left(g v^* \right)^{rnc} \left(\tilde{v}^{1/3} - 1 \right)^{3rnc} \exp \left(rnc / \tilde{v} \tilde{T} \right). \quad (3.44)$$

Here, Z_{comb} is a combinatory factor, g is an inconsequential geometric factor, v^* is a characteristic (specific) volume per segment (usually called the hard-core or closed-packed volume), \tilde{v} is a reduced volume per segment defined in terms of the characteristic volume, r is the mean number of segments per molecule, n is the number of molecules (or mers), c is the mean number of external degrees of freedom per segment,* and \tilde{T} is a reduced temperature as defined later. The exponential term in eq. (3.44) is related to the configurational or mean potential energy (in van der Waals form), which is inversely proportional to volume.

Statistical thermodynamics provides the following equation to obtain an EOS from the partition function:

$$p = kT \left(\frac{\partial \ln Z}{\partial V} \right)_T. \quad (3.45)$$

The resulting EOS obtained from the partition function given by eq. (3.44) can be expressed in reduced form as

$$\boxed{\frac{\tilde{p}\tilde{v}}{\tilde{T}} = \frac{\tilde{v}^{1/3}}{\tilde{v}^{1/3} - 1} - \frac{1}{\tilde{T}\tilde{v}}} \quad (3.46)$$

* The total number of degrees of freedom in the system is $3rnc$.

where \tilde{p} is the reduced pressure. The reduced parameters are defined in terms of the characteristic parameters (three EOS parameters, v^* , T^* , and p^* , for each of the pure components) as

$$\tilde{v} = \frac{v}{v^*}, \quad (3.47)$$

$$\tilde{T} = \frac{T}{T^*} = \frac{2v^* cRT}{s\eta}, \quad (3.48)$$

and

$$\tilde{p} = \frac{p}{p^*} = \frac{2pv^{*2}}{s\eta}, \quad (3.49)$$

where c represents the mean number of external degrees of freedom per segment, s is the number of contact sites per segment, and η is an energy parameter characterizing a pair of sites in contact. The characteristic parameters can be obtained from experimental PVT data.* Representative values for Flory EOS parameters evaluated

* Differentiation of the EOS (eq. (3.46)) with respect to temperature at constant pressure yields at zero pressure the characteristic hard-core volume as

$$v^* = v \left[\frac{3 + 3\alpha T}{3 + 4\alpha T} \right]^3.$$

Differentiation of the EOS with respect to temperature at constant volume yields at zero pressure the characteristic pressure

$$p^* = \gamma T \tilde{v}^2 = (\alpha / \beta) \tilde{T}^2$$

where α is the *thermal-expansion coefficient*

$$\alpha = \frac{1}{V} \left(\frac{\partial V}{\partial T} \right)_p,$$

β is the *compressibility coefficient*

$$\beta = -\frac{1}{V} \left(\frac{\partial V}{\partial p} \right)_T,$$

and γ is the *thermal-pressure coefficient*

$$\gamma = \left(\frac{\partial p}{\partial T} \right)_V.$$

Finally, the characteristic temperature is obtained from the EOS by letting $\tilde{p} = 0$:

at 25°C for four low-molecular-weight organic compounds and for four polymers are given in Table 3-2. In general, v^* and T^* increase with increasing temperature while p^* decreases.

Table 3-2 Flory Equation-of-State Parameters at 25°C

Polymer	v^* (cm ³ g ⁻¹)	T^* (K)	p^* (J cm ⁻³)
Benzene	0.8860	4709	628
Cyclohexane	1.0012	4721	530
Methyl ethyl ketone	0.9561	4555	582
Toluene	0.9275	5197	547
Natural rubber	0.9432	6775	519
Polydimethylsiloxane	0.8395	5530	241
Polyisobutylene	0.9493	7580	448
Polystyrene	0.8098	7420	547

Adaptation of the Flory EOS to *mixtures* is based upon the following two premises:

1. Core volumes of the solution components are additive. For example, the hard-core volume of a binary mixture is given as

$$v^* = \frac{n_1 v_1^* + n_2 v_2^*}{n_1 + n_2}. \quad (3.50)$$

2. The intermolecular energy depends on the *surface area* of contact between molecules and/or segments.

Since a segment is an arbitrary unit, the segment size can be chosen such that $v_1^* = v_2^* = v^*$. This gives the following mixing rules for the binary mixture:

$$\frac{1}{r} = \frac{\phi_1}{r_1} + \frac{\phi_2}{r_2} \quad (3.51)$$

where ϕ_1 and ϕ_2 are *segment* (or *core-volume*) *fractions*:

$$\phi_1 = 1 - \phi_2 = \frac{n_1 v_1^*}{n_1 v_1^* + n_2 v_2^*}. \quad (3.52)$$

The *number of contact sites*, s , for the mixture is given as

$$T^* = \frac{T \tilde{v}^{4/3}}{\tilde{v}^{1/3} - 1}.$$

$$s = \phi_1 s_1 + \phi_2 s_2 \quad (3.53)$$

where s_i is the *surface area* of a segment of component i . In a similar manner, the mean number of external degrees of freedom for the mixture can be written as

$$c = \phi_1 c_1 + \phi_2 c_2. \quad (3.54)$$

The *site fraction* is defined as

$$\theta_2 = 1 - \theta_1 = \frac{\phi_2 s_2}{s}. \quad (3.55)$$

The *characteristic pressure* for the mixture is given as

$$p^* = \phi_1 p_1^* + \phi_2 p_2^* = \phi_1 \theta_2 X_{12} \quad (3.56)$$

where X_{12} is called the *exchange interaction parameter*, defined as

$$X_{12} = \frac{s_1(\eta_{11} + \eta_{22} - 2\eta_{12})}{2v^{*2}} = \frac{s_1 \Delta \eta}{2v^{*2}} \quad (3.57)$$

where the η_{ij} terms are energy parameters for the $i-j$ segment pairs and $\Delta \eta = \eta_{11} + \eta_{22} - 2\eta_{12}$. The exchange interaction parameter is analogous to $\Delta \omega_{12}$ in the Flory–Huggins theory (i.e., eq. (3.32)) but has the dimensions of energy density. Finally, the *characteristic temperature* for the mixture is given as

$$T^* = \frac{\phi_1 p_1^* + \phi_2 p_2^* - \phi_1 \theta_2 X_{12}}{\frac{\phi_1 p_1^*}{T_1^*} + \frac{\phi_2 p_2^*}{T_2^*}}. \quad (3.58)$$

The EOS of the mixture is given in the same form as that of the pure component (eq. (3.46)) except that the reduced parameters refer to those of the mixture. The reduced volume of the mixture, \tilde{v} , may be obtained from the EOS with \tilde{p} set to zero for low pressures and \tilde{T} defined by use of the characteristic temperature given by eq. (3.58) for the mixture. Subsequently, other important quantities can be calculated such as the molar enthalpy of mixing as

$$\Delta H_m = \frac{\theta_2 x_1 v_1^* X_{12}}{\tilde{v}} + x_1 v_1^* p_1^* \left(\frac{1}{\tilde{v}_1} - \frac{1}{\tilde{v}} \right) + x_2 v_2^* p_2^* \left(\frac{1}{\tilde{v}_2} - \frac{1}{\tilde{v}} \right) \quad (3.59)$$

where

$$x_1 = \frac{n_1}{n_1 + n_2}. \quad (3.60)$$

An important relationship is the Flory EOS expression for $\Delta\mu_1$ given as

$$\Delta\mu_1 = RT \left[\ln \phi_1 + \left(1 - \frac{\nu_1^*}{\nu_2^*} \right) \phi_2 \right] + \frac{\theta_2^2 \nu_1^* X_{12}}{\tilde{v}} + \nu_1^* p_1^* \left[3\tilde{T}_1 \ln \left(\frac{\tilde{v}_1^{1/3} - 1}{\tilde{v}^{1/3} - 1} \right) + \frac{1}{\tilde{v}_1} - \frac{1}{\tilde{v}} \right]. \quad (3.61)$$

Alternatively, eq. (3.61) has been given in the form

$$\begin{aligned} \Delta\mu_1 = RT & \left(\ln \phi_1 + \frac{1 - r_1}{r_2} \phi_2 \right) + p_1^* \nu_1^* \left[3\tilde{T}_1 \ln \left(\frac{\tilde{v}_1^{1/3} - 1}{\tilde{v}^{1/3} - 1} \right) + \tilde{v}_1^{-1} - \tilde{v}^{-1} + \tilde{p}_1 (\tilde{v} - \tilde{v}_1) \right] \\ & + (X_{12} - TQ_{12}\tilde{v}) \nu_1^* \frac{\theta_2^2}{\tilde{v}}. \end{aligned} \quad (3.62)$$

A principal difference between eqs. (3.61) and (3.62) is the appearance of Q_{12} in the last term of eq. (3.62). This parameter is called the *non-combinational entropy correction* and generally is used as an adjustable parameter. Comparison of the standard Flory–Huggins relationship (eq. (3.36), where $\Delta\mu_1 = RT \ln a_1$ and $\phi_1 = 1 - \phi_2$) with the Flory EOS (eq. (3.61)) shows that the first term within brackets in eq. (3.61) is simply a combinatory term. Despite its cumbersome form, the Flory EOS theory provides substantial improvement over the earlier lattice theory. For example, the theory reasonably predicts an excess volume of mixing as

$$\frac{V^E}{V} = \frac{\nu^E}{\tilde{v}} = 1 - \frac{\phi_1 \tilde{v}_1 + \phi_2 \tilde{v}_2}{\tilde{v}}. \quad (3.63)$$

Furthermore, it is capable of modeling the complete range of the observed phase behavior of polymer solutions, as discussed in the next section.

3.2.4 Phase Equilibria

Whether or not a polymer and solvent are mutually soluble, or *miscible*, is governed by the sign of the Gibbs free energy of mixing, ΔG_m , which is related to the enthalpy and entropy of mixing by eq. (3.28). Three different dependencies of ΔG_m on solution composition (i.e., volume fraction of polymer) at constant temperature are illustrated in Figure 3-9. If ΔG_m is positive over the entire composition range, as illustrated by curve I, the polymer and solvent are totally immiscible over the complete composition range and will coexist at equilibrium as two distinct phases. Two other possibilities are those of partial and total miscibility, as illustrated by curves II and III, respectively. For total miscibility, it is *necessary* that

$$\Delta G_m < 0 \quad (3.64)$$

and that the second derivative of ΔG_m with respect to the volume fraction of solvent (component 1) or polymer (component 2) be greater than zero over the entire composition range as formally expressed by

$$\left(\frac{\partial^2 \Delta G_m}{\partial \phi_2^2} \right)_{p,T} > 0. \quad (3.65)$$

Both conditions for miscibility are satisfied by curve III but not curve II, which exhibits two minima in ΔG_m , and therefore the derivative criterion expressed by eq. (3.65) is not satisfied at all points along the ΔG_m -composition curve. A solution that exhibits such minima will phase-separate at equilibrium into two phases containing different compositions of both components. The compositions of the two phases are given by the points of common tangent as illustrated in Figure 3-9, where the composition of the solvent-rich phase is identified as ϕ_2^A and that of the polymer-rich phase as ϕ_2^B .

Phase equilibrium is strongly affected by solution temperature. In fact, any of three types of phase behavior illustrated in Figure 3-9 may result from a change in the temperature (or pressure) of the system. Our usual experience with solutions of low-molecular-weight compounds is that solubility increases with an increase in temperature, as illustrated by the phase diagram shown in Figure 3-10. In this example, the solution is homogeneous (i.e., the two components are totally miscible) at temperatures above the point identified as UCST, which stands for the *upper critical solution temperature* as described below. At lower temperatures (i.e., below the UCST), phase separation may occur depending upon the overall composition of the mixture. At a given temperature below the UCST (e.g., T_1), compositions lying *outside* the curves are those constituting a homogeneous phase, while those lying *inside* the curves are thermodynamically unstable and, therefore, the solution will phase-separate at equilibrium. The compositions of the two phases, identified as phases A and B, are given by points lying along the curve called the *binodal*. The binodal is the locus of points that satisfy the conditions for thermodynamic equilibrium of a binary mixture given as

$$\mu_1^A = \mu_1^B \quad (3.66)$$

and

$$\mu_2^A = \mu_2^B. \quad (3.67)$$

As the chemical potential is given by the derivative of the Gibbs free energy with respect to composition (eq. (3.29)), the chemical potentials are obtained graphically from the intercepts of the common tangent drawn to curve II with the free energy axes as illustrated in Figure 3-9.

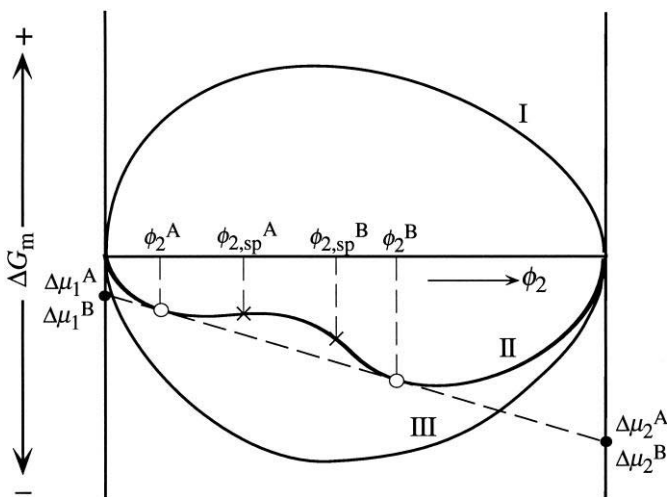


Figure 3-9 Dependence of the Gibbs free energy of mixing, ΔG_m , of a binary mixture on volume fraction of polymer, ϕ_2 , at constant pressure and temperature. **I.** Total immiscibility. **II.** Partial miscibility. **III.** Total miscibility. In the case of partial miscibility (curve II), the mixture will separate into two phases whose compositions (\circ) are marked by the volume-fraction coordinates, ϕ_2^A and ϕ_2^B , corresponding to points of common tangent to the free-energy curve. Spinodal points, compositions $\phi_{2,sp}^A$ and $\phi_{2,sp}^B$, occur at the points of inflection (\times).

Between the binodal and the unstable region lies the *metastable* region, which is bounded by the *spinodal*. In the metastable region, the system can resist small concentration fluctuations but will eventually equilibrate to the stable two-phase state given by the binodal. Points lying along the spinodal correspond to the points of inflection identified in curve II of the free-energy diagram (Figure 3-9) and satisfy the relationship

$$\left(\frac{\partial^2 \Delta G_m}{\partial \phi_2^2} \right)_{p,T} = 0 . \quad (3.68)$$

The binodal and spinodal coincide at the *critical point*, which satisfies the following equality for the third derivative of the Gibbs free energy with respect to composition:

$$\left(\frac{\partial^3 \Delta G_m}{\partial \phi_2^3} \right)_{p,T} = 0 . \quad (3.69)$$

In the case of the upper critical solution temperature (UCST), the critical point lies at the top of the phase diagram as shown in Figure 3-10.

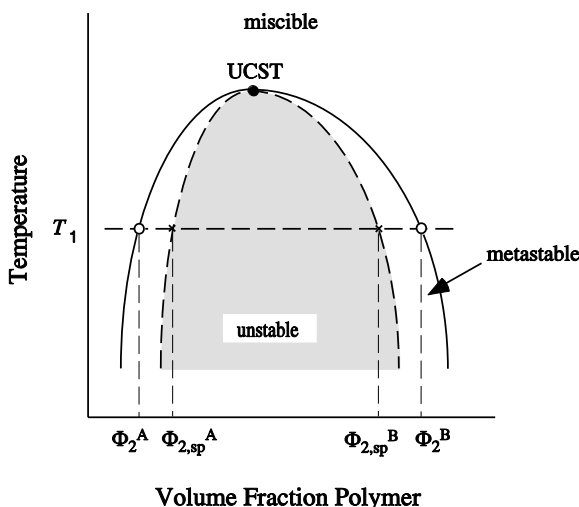


Figure 3-10 Representative phase diagrams for a polymer solution showing an upper critical solution temperature (UCST) (○), spinodal curve (— · —), and binodal curve (—).

Although the UCST behavior of dilute polymer solutions had been observed for many years, it was not until 1961 that phase separation of polymer solutions was first reported to occur with an *increase* in temperature [17]. In this case, the binodal and spinodal curves coincide at a temperature and composition called the *lower critical solution temperature* or LCST. One serious limitation of the Flory–Huggins theory (Section 3.2.1) is that it fails to predict LCST behavior. The more recent equation-of-state theories (Section 3.2.3) are much more successful in predicting the entire range of phase behavior, as will be discussed in Section 7.2.

3.2.5 Determination of the Interaction Parameter

Experimentally, χ_{12} as well as the exchange interaction parameter, X_{12} , in the Flory EOS theory can be determined by a variety of techniques, including several scattering methods as discussed in the next section and from the melting-point depression of semicrystalline polymers (see Section 4.2.2). A commonly used method to determine polymer–solvent as well as polymer–polymer interaction parameters (Chapter 7) has been inverse gas chromatography or IGC [18] as described in the following section.

Inverse Gas Chromatography. The term *inverse* is used to indicate that the substance being characterized constitutes the stationary phase (i.e., the bed packing) rather than the mobile phase, as is the case in traditional gas chromatography. The stationary phase is prepared by coating a thin layer of a polymer or polymer blend from a dilute solution onto a commercial packing material in the form of small beads. A fluidized bed is sometimes used in the coating process. The coated packing is vacuum-dried to remove all residual solvent and then packed into a GC column that is heated to approximately 50°C above the glass-transition temperature (T_g). A solvent probe is then injected into the carrier gas (He or H₂), and the time for the probe to be eluted from the column is measured. During its passage, the probe is free to be sorbed into the liquid polymer coating of the packed bed. The extent of solubility (i.e., activity) is directly related to the retention time from which a *specific retention volume*, V_g , can be calculated. From this value, the infinite-dilution volume-fraction activity coefficient is then obtained as [19]

$$\ln \gamma_1^\infty = \ln \left(\frac{a_1}{\phi_1} \right)^\infty = \lim_{\phi_1 \rightarrow 0} \left(\frac{a_1}{\phi_1} \right) = \ln \left(\frac{273.16 R v_2}{V_g p_1^\circ} \right) - \frac{p_1^\circ (B_{11} - V_1)}{RT} \quad (3.70)$$

where ϕ_1 is the volume fraction of solvent (probe), p_1° is the vapor pressure of the probe (solvent) in the carrier gas, v_2 is the specific volume of the polymer, V_1 is the molar volume of the probe, and B_{11} is the second virial coefficient of the pure probe vapor at the measurement temperature. From the measurement of γ_1^∞ at different temperatures, the heat of mixing can be determined as

$$\Delta H_m = R \left[\frac{\partial \ln \gamma_1^\infty}{\partial (1/T)} \right]. \quad (3.71)$$

From eq. (3.70) and the Flory–Huggins equation (eq. (3.37)), it is easily shown that the Flory interaction parameter is obtained directly as

$$\chi_{12} = \ln \left(\frac{273.16 R v_2}{V_g p_1^\circ V_1} \right) - \frac{p_1^\circ (B_{11} - V_1)}{RT} - 1. \quad (3.72)$$

In a similar manner, the interaction energy, X_{12} , in the Flory equation of state also can be obtained (see Problem 3.11).

3.2.6 Predictions of Solubilities

Solubility Parameters. As discussed in the previous section, there are a number of experimental methods by which approximate values of χ_{12} can be obtained; howev-

er, there is no theory by which values of χ_{12} can be *predicted* at the present time. One approach that can be used to estimate χ_{12} and predict solubility is based upon the concept of the *solubility parameter*, δ , which was originally developed to guide solvent selection in the paint and coatings industry. The solubility parameter is related to the cohesive energy density, E^{coh} , or the molar energy of vaporization of a pure liquid, ΔE^{v} , as

$$\delta_i = \sqrt{E_i^{\text{coh}}} = \sqrt{\frac{\Delta E_i^{\text{v}}}{V_i}} \quad (3.73)$$

where ΔE^{v} is defined as the energy change upon isothermal vaporization of the saturated liquid to the ideal gas state at infinite dilution* and V_i is the molar volume of the liquid. Units of δ are $(\text{cal cm}^{-3})^{1/2}$ or $(\text{MPa})^{1/2}$.[†] Equation (3.73) can be used to calculate the solubility parameter of a pure solvent given values of ΔE^{v} and V_i . Since it is not reasonable to talk about an energy of vaporization for solid polymers, the solubility parameter of a polymer has to be determined indirectly or calculated by group-contribution methods. Experimentally, the solubility parameter of a polymer can be estimated by comparing the swelling of a crosslinked polymer sample immersed in different solvents. The solubility parameter of the polymer is taken to be that of the solvent resulting in maximum swelling. Alternatively, the solubility parameter can be estimated by use of group-contribution methods as discussed in Section 13.1.4. An additional approach that can be used to calculate δ is based upon knowledge of the equation of state, $V(p, T)$, for the polymer [20]

$$\delta \cong \sqrt{\frac{T\alpha}{\beta}} \quad (3.74)$$

where α is the (isobaric) thermal-expansion coefficient,

$$\alpha = \left(\frac{1}{V} \right) \left(\frac{\partial V}{\partial T} \right)_p , \quad (3.75)$$

and β is the (isothermal) compressibility coefficient,[‡]

* The energy of vaporization is approximately related to the enthalpy of vaporization as

$$\Delta E_i^{\text{v}} = \Delta H_i^{\text{v}} - RT.$$

[†] 1 $(\text{cal cm}^{-3})^{1/2} = 2.045 (\text{MPa})^{1/2}$.

[‡] Since volume *decreases* with increasing pressure, the negative sign in eq. (3.76) provides a positive value for β .

$$\beta = -\left(\frac{1}{V}\right) \left(\frac{\partial V}{\partial P} \right)_T . \quad (3.76)$$

Equations of state are now available for most commercial polymers [21, 22].

From values of the solubility parameters for the solvent and polymer, the heat of mixing can be estimated by the Scatchard [23]–Hildebrand [24] equation as

$$\Delta H_m = V (\delta_1 - \delta_2)^2 \phi_1 \phi_2 \quad (3.77)$$

where V is the volume of the mixture. Making use of eq. (3.34), the interaction parameter can be estimated from this value of ΔH_m as*

$$\boxed{\chi_{12} \cong \frac{V_1}{RT} (\delta_1 - \delta_2)^2} \quad (3.78)$$

where V_1 is the molar volume of component 1. As the form of eq. (3.77) indicates, the solubility parameter approach can be used to estimate the heat of mixing when $\Delta H_m \geq 0$ but not when $\Delta H_m < 0$ (i.e., for exothermic heat of mixing).

The matching of polymer and solvent solubility parameters to minimize ΔH_m is a useful approach for solvent selection in many cases but often fails when specific interactions such as hydrogen bonding occur. To improve the prediction, two- and three-dimensional solubility parameters, which give individual contributions for dispersive (i.e., van der Waals), polar, and hydrogen-bonding interactions, are sometimes used. In the case of the three-dimensional model proposed by Hansen [25], the overall solubility parameter can be obtained as

$$\delta = \sqrt{\delta_d^2 + \delta_p^2 + \delta_h^2} \quad (3.79)$$

where δ_d , δ_p , and δ_h are the dispersive, polar, and hydrogen-bonding solubility parameters, respectively. Values of δ calculated from eq. (3.79) for common solvents and polymers are given in Table 3-3.

* Sometimes, the Flory interaction parameter is considered to have both an enthalpic component, χ_H , and entropic (or residual) component, χ_S . In this case, we can write

$$\chi_{12} = \chi_S + \chi_H = \chi_S + \frac{V_1}{RT} (\delta_1 - \delta_2)^2 \approx 0.34 + \frac{V_1}{RT} (\delta_1 - \delta_2)^2 .$$

Table 3-3 Solubility Parameters of Some Common Solvents and Polymers

	Solubility Parameter, δ^a (MPa) $^{1/2}$	Solubility Parameter, δ^a (cal cm $^{-3}$) $^{1/2}$
Solvents		
<i>n</i> -Hexane	14.9	7.28
Carbon tetrachloride	17.8	8.70
Toluene	18.2	8.90
Benzene	18.6	9.09
Chloroform	19.0	9.29
Tetrahydrofuran	19.4	9.48
Chlorobenzene	19.6	9.58
Methylene chloride	20.3	9.92
1,4-Dioxane	20.5	10.0
<i>N</i> -Methyl-2-pyrrolidone	22.9	11.2
Dimethylformamide	24.8	12.1
Methanol	29.7	14.5
Water	47.9	23.4
Polymers		
Polyisobutylene	15.5	7.58
Polysulfone	20.3	9.92
Poly(vinyl chloride)	21.5	10.5
Polystyrene	22.5	11.0
Poly(methyl methacrylate)	22.7	11.1
Cellulose acetate	25.1	12.3
Polyacrylonitrile	25.3	12.4
Poly(vinyl acetate)	25.7	12.7

^a Calculated from Hansen solubility parameters using eq. (3.79) at 25°C; conversion: 1 MPa $^{1/2}$ = 0.489 (cal cm $^{-3}$) $^{1/2}$.

3.3 MEASUREMENT OF MOLECULAR WEIGHT

As discussed in Section 1.3, commercial polymers have broad distributions of molecular weights, and it is, therefore, necessary to report an average molecular weight when characterizing a sample. There are three important molecular-weight averages—number-average (\bar{M}_n), weight-average (\bar{M}_w), and *z*-average (\bar{M}_z). Absolute values of \bar{M}_n , \bar{M}_w , and \bar{M}_z can be obtained by the *primary* characterization methods of osmometry, scattering, and sedimentation, respectively. In addition to these accurate but time-consuming techniques, there are a number of *secondary* methods by which average molecular weights can be determined provided that polymer samples with narrow molecular-weight distributions are available for reference and calibration. The most important of these secondary methods is gel-permeation chromatography (GPC), sometimes called size-exclusion chromatography (SEC). This

method is capable of determining the entire molecular-weight distribution of a polymer sample from which all molecular-weight averages can be determined. Another widely used secondary method is the determination of intrinsic viscosity from which the viscosity-average molecular weight can be determined. The viscosity-average molecular weight (\bar{M}_v) normally lies between \bar{M}_n and \bar{M}_w . The principles behind both primary and secondary methods for molecular-weight determination are discussed next.

3.3.1 Osmometry

Membrane Osmometry. The osmotic pressure, Π , of a polymer solution may be obtained from the chemical potential, $\Delta\mu_1$, or equivalently from the activity, a_1 , of the solvent through the basic relationship

$$\Delta\mu_1 = RT \ln a_1 = -\Pi V_1 \quad (3.80)$$

where V_1 is the molar volume of the solvent. Substitution of the Flory–Huggins expression for solvent activity (eq. (3.37)) into eq. (3.80) and subsequent rearrangement give

$$\Pi = -\frac{RT}{V_1} [\ln(1 - \phi_2) + \phi_2 + \chi_{12}\phi_2^2]. \quad (3.81)$$

Simplification of this relation can be achieved by expansion of the logarithmic term in a Taylor series (see Appendix E) and the substitution of polymer concentration, c , for volume fraction, ϕ_2 , through the relationship

$$\phi_2 = cv \quad (3.82)$$

where v is the specific volume of the polymer. Substitution and rearrangement give the expression

$$\frac{\Pi}{c} = \frac{RT}{M} \left[1 + \left(\frac{Mv^2}{V_1} \right) \left(\frac{1}{2} - \chi_{12} \right) c + \frac{1}{3} \left(\frac{Mv^3}{V_1} \right) c^2 + \dots \right]. \quad (3.83)$$

The classical van't Hoff equation for the osmotic pressure of an ideal solution

$$\frac{\Pi}{c} = \frac{RT}{M} \quad (3.84)$$

may be seen as a special or limiting case of eq. (3.83) obtained when $\chi_{12} = 1/2$ and second- and higher-order terms in c can be neglected (i.e., for dilute solution). For high-molecular-weight, polydisperse polymers, the appropriate molecular weight to

use in eq. (3.83) is the number-average molecular weight, \bar{M}_n . Equation (3.83) can then be rearranged to give the widely used relation

$$\boxed{\Pi = RTc \left(\frac{1}{\bar{M}_n} + A_2 c + A_3 c^2 + \dots \right)} \quad (3.85)$$

where A_2 and A_3 are the second and third virial coefficients, respectively. Comparison of eqs. (3.83) and (3.85) reveals the following two relations for the virial coefficients:

$$A_2 = \frac{V^2}{V_1} \left(\frac{1}{2} - \chi_{12} \right) \quad (3.86)$$

$$A_3 = \frac{1}{3} \left(\frac{V^3}{V_1} \right). \quad (3.87)$$

In the limit of dilute solution (typically less than 1 g dL⁻¹), terms containing second- and higher-order powers of c can be neglected, and therefore a plot of Π/RTc versus c yields a straight line with an intercept, $1/\bar{M}_n$, and slope, A_2 . In Figure 3-11, plots of osmotic data for different molecular-weight fractions of polyisobutylene in a good (cyclohexane) and poor (benzene) solvent are compared.

As shown by the relation between A_2 and χ_{12} given by eq. (3.86), the second virial coefficient is a convenient measure of the *quality* of polymer–solvent interactions. In good solvents in which the polymer chains are expanded (i.e., $\alpha > 1$, eq. (3.13)), A_2 is large and, therefore, χ_{12} is small (e.g., <0.5). At θ conditions (i.e., $\alpha = 1$), $A_2 = 0$ and $\chi_{12} = 0.5$.

Experimental procedures to determine osmotic pressure are relatively simple although often very time-consuming. A basic osmometer design is illustrated in Figure 3-12. In operation, pure solvent and a dilute solution of the polymer in the same solvent are placed on opposite sides of a semipermeable membrane, typically prepared from cellulose or a cellulose derivative. Regenerated cellulose is an especially good membrane polymer because it is insoluble in most organic solvents. Normally, the membrane is first preconditioned in the solvent used in the measurements. An ideal membrane will allow the solvent to pass through the membrane but will retain the polymer molecules in solution. The resulting difference in chemical potential between solvent and the polymer solution causes solvent to pass through the membrane and raise the liquid head of the solution reservoir. The osmotic pressure is calculated from the height, h , of the equilibrium head representing the difference between the height of solvent in the solvent capillary and the height of solution in the opposite capillary at equilibrium as

$$\Pi = \rho g h. \quad (3.88)$$

where ρ is the solvent density and g is the gravitational acceleration (9.8066 m s^{-2}).

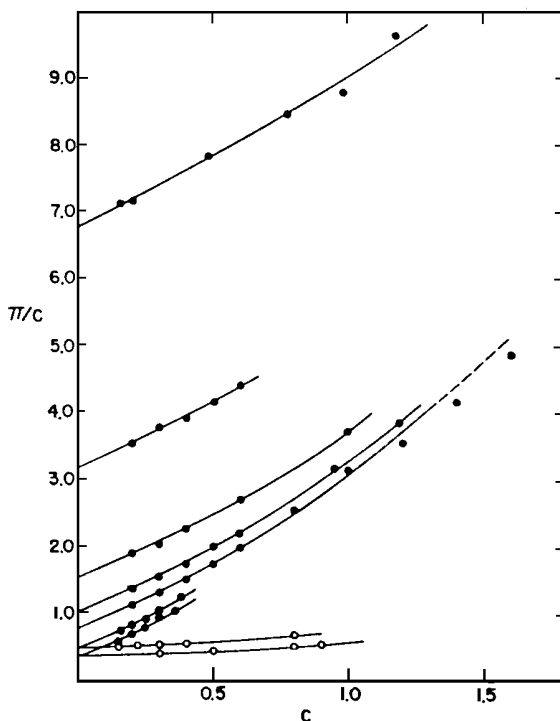


Figure 3-11 Plot of Π/c versus c (g cm^{-3}) for polyisobutylene fractions (molecular weights ranging from 38,000 and 720,000) in benzene (\circ) and in cyclohexane (\bullet). Adapted with permission from W. R. Krigbaum and P. J. Flory, *Statistical Mechanics of Dilute Polymer Solutions. IV. Variation of the Osmotic Second Coefficient with Molecular Weight*. Journal of the American Chemical Society, 1953. **75**(8): p. 1775–1784.

One intrinsic problem with membrane osmometry is the performance of the membrane. No membrane is completely impervious to the passage of small molecules, and any migration of smaller polymer molecules across the membrane during measurement will not contribute to the osmotic pressure and, therefore, an artificially high value of \bar{M}_n will be obtained. For this reason, membrane osmometry is accurate only for polymer samples with molecular weights above about 20,000. The upper limit for molecular weight is approximately 500,000 due to inaccuracy in measuring small osmotic pressures. For the characterization of low-molecular-weight (i.e., $<20,000$) oligomers and polymers, an alternative technique called vapor-pressure osmometry (VPO) is preferred, particularly when molecular weight is less than about 10,000. The basic principles of this technique are described next.

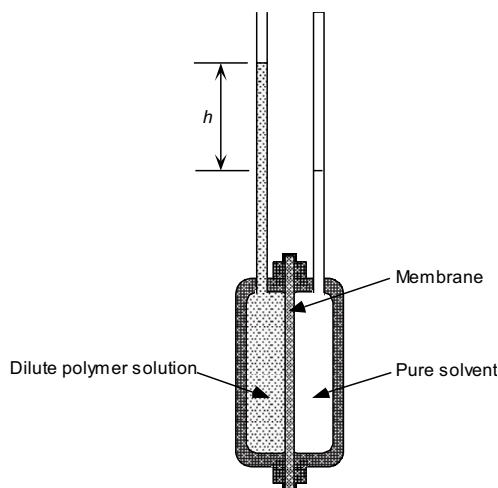


Figure 3-12 Schematic of a simple membrane osmometer.

Vapor-Pressure Osmometry. When a polymer is added to a solvent, the vapor pressure of the solvent will be lowered due to the decrease in solvent activity. The relation between the difference in vapor pressure between solvent and solution, $\Delta p (= p_1 - p_1^\circ)$, and the number-average molecular weight, \bar{M}_n , of the polymer is given as

$$\lim_{c \rightarrow 0} \left(\frac{\Delta p}{c} \right) = -\frac{p_1^\circ V_1^\circ}{\bar{M}_n} \quad (3.89)$$

where p_1° and V_1° are, respectively, the vapor pressure and molar volume of the pure solvent. Due to the inverse dependence of Δp on \bar{M}_n given by eq. (3.89), the effect of even a low-molecular-weight polymer on the lowering of vapor pressure will be very small and, therefore, direct measurement of the vapor pressure is a very imprecise method of molecular-weight determination. For this reason, an indirect approach, based upon thermoelectric measurements, is used in commercial instrumentation as described below.

As shown by Figure 3-13, a commercial vapor-pressure osmometer uses two matched thermistors that are placed in a closed, constant-temperature ($\pm 0.001^\circ\text{C}$) chamber containing saturated solvent vapor. A drop of solvent is placed by syringe on one thermistor and a drop of dilute polymer solution on the other. As a result of condensation of solvent vapor onto the solution, the temperature of the solution thermistor increases until the vapor pressure of the solution equals that of the solvent. The difference in temperature between the two thermistors is recorded in terms of a difference in resistance (ΔR), which is calibrated by use of a standard

low-molecular-weight sample. Extrapolation of $\Delta R/c$ over a range of dilute-solution concentrations to zero concentration yields M_n through

$$\left(\frac{\Delta R}{c} \right)_{c \rightarrow 0} = \frac{K_{VPO}}{M_n} \quad (3.90)$$

where K_{VPO} is the calibration constant obtained by measuring ΔR for a low-molecular-weight standard whose molecular weight is precisely known. As in membrane osmometry, the slope of the plot of $\Delta R/c$ versus c is related to the second virial coefficient. Criteria for the selection of calibrants for VPO include high purity (>99.9%) and low vapor pressure (<0.1% of p_1^0). Examples of calibrant include mannitol and sucrose for aqueous solution measurements and pentaerythritol tetraesteate, and low-polydispersity, low-molecular-weight polystyrene and polyisobutylene standards for organic-solution determinations. Since calibration by a low-molecular-weight standard is required to obtain K_{VPO} , VPO is considered a secondary method of molecular-weight determination, in contrast to membrane osmometry for which no calibration is required.

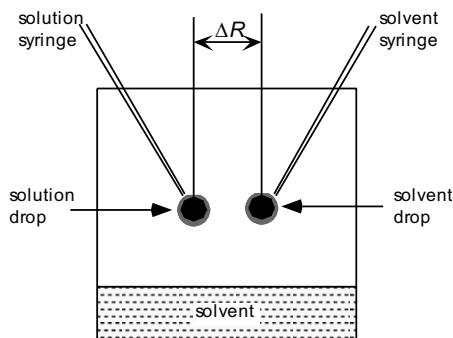


Figure 3-13 Illustration of basic instrumentation for vapor-pressure osmometry.

3.3.2 Light-Scattering Methods

The weight-average molecular weight can be obtained directly only from scattering measurements. The most commonly used technique is light scattering from dilute polymer solution. It is also possible to determine M_w by small-angle neutron scattering of specially prepared solid samples. Although this technique has great current importance in polymer research, it is not routinely used for molecular-weight determination because of the difficulty and expense of sample preparation and the

specialized facilities required. The basic principles of light-scattering measurements of dilute polymer solutions are described next.

The fundamental relationship for light scattering is given as^{*}

$$\boxed{\frac{Kc}{R(\theta)} = \frac{1}{\bar{M}_w P(\theta)} + 2A_2 c + \dots} \quad (3.91)$$

In this equation, K is a function of the refractive index, n_o , of the pure solvent, the specific refractive increment, dn/dc , of the dilute polymer solution, and the wavelength, λ , of the incident light according to the relationship

$$K = \frac{2\pi^2 n_o^2}{N_A \lambda^4} \left(\frac{dn}{dc} \right)^2 \quad (3.92)$$

where N_A is Avogadro's number (6.023×10^{23} molecules mol⁻¹). The specific refractive increment is the change in refraction index, n , of dilute polymer solutions with increasing polymer concentration. The term $R(\theta)$ appearing in eq. (3.91) is called the *Rayleigh ratio* defined as

$$R(\theta) = \frac{i(\theta)r^2}{I_o V}. \quad (3.93)$$

In this equation, I_o is the intensity of the incident light beam and $i(\theta)$ is the intensity of the *scattered* light measured at a distance of r from the scattering volume, V , and at an angle θ with respect to the incident beam. The parameter $P(\theta)$ appearing in eq. (3.91) is called the *particle-scattering function*, which incorporates the effect of chain size and conformation on the angular dependence of scattered light intensity, as illustrated in Figure 3-15. Spherical particles having dimensions smaller than the wavelength of light act as independent scattering centers generating a symmetrical envelope of scattered light intensity. In the case of small particles, $P(\theta)$ is unity, but in the case of polymer chains whose dimensions are $>\lambda/20$, scattering may occur from different points along the same chain and $P(\theta) < 1$. For this reason, diminution of scattered light intensity can occur due to interference, and the scattering envelope is no longer spherically symmetrical, as seen in Figure 3-14. In this case, the angular dependence of scattered light intensity is given by the particle-scattering func-

^{*} It can be shown from the thermodynamic theory of fluctuations that the relationship between scattered light intensity and chemical potential is given as

$$R(\theta) = \frac{KcRTV_1(1 + \cos^2 \theta)}{-\partial \mu / \partial c} = \frac{KcRTV_1(1 + \cos^2 \theta)}{\partial \Pi / \partial c}.$$

tion, which, for a *monodisperse* system of randomly coiling molecules in dilute solution, is given by the expression

$$P(\theta) = \frac{2}{v^2} [e^{-v} - (1-v)] \quad (3.94)$$

where

$$v = 16 \left(\frac{\pi n}{\lambda} \right)^2 \langle s^2 \rangle \sin^2 \left(\frac{\theta}{2} \right) \quad (3.95)$$

and $\langle s^2 \rangle$ is called the mean-square radius of gyration. For linear-chain polymers, $\langle s^2 \rangle$ is related to the mean-square end-to-end distance as

$$\langle s^2 \rangle = \frac{\langle r^2 \rangle}{6}. \quad (3.96)$$

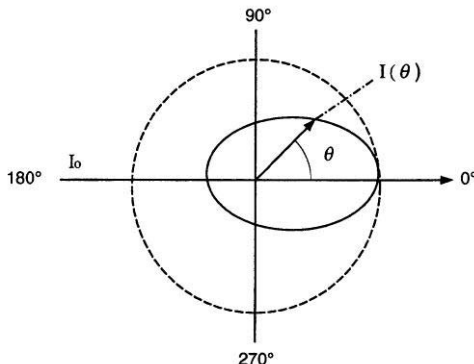


Figure 3-14 Intensity distribution of light scattering at various angles for a small particle (dashed circle) and a large polymer molecule (solid ellipse).

Basic instrumentation for light-scattering measurements is illustrated in Figure 3-15. Light from a high-intensity mercury lamp is polarized and filtered before passing through a glass cell that contains a filtered, dilute polymer solution. Scattered light intensity at an angle θ is recorded as a signal from a movable high-voltage photomultiplier tube.

To determine M_w from eq. (3.91), it is necessary to know the value of $P(\theta)$ at each angle for which $R(\theta)$ has been measured. When the molecular-weight distribution of a polymer is polydisperse, as it usually is, $P(\theta)$ is not precisely given by eq. (3.94), but by a summation of similar equations for polymer chains of different sizes weighted by the amount of variously sized chains present in the polymer sample.

Since this information is generally not known, it is customary to treat the data in a way that does not require explicit knowledge of $P(\theta)$. In practice, two approaches can be used. These are called the *Zimm* and *dissymmetry* methods, which are discussed in the following sections.

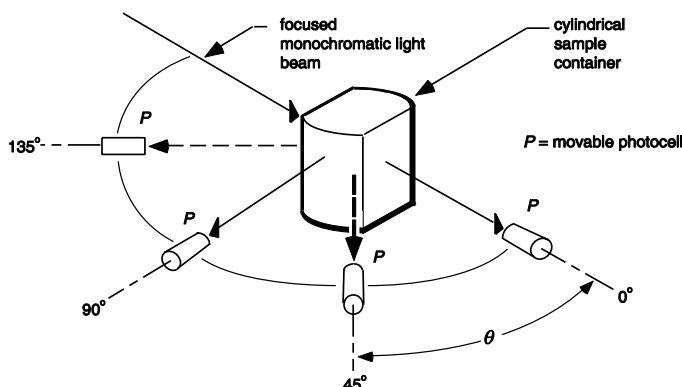


Figure 3-15 Conventional light-scattering instrumentation. From F. Rodriguez, *Principles of Polymer Systems*. 2003. Reproduced with permission of Routledge Publishing, Inc., in book format via Copyright Clearance Center.

Zimm Method. The most rigorous approach to determine \bar{M}_w from light-scattering data is a *Zimm plot*. This procedure has the advantage that chain conformation need not be known in advance; however, Zimm plots require tedious measurements of scattered light intensity at many more angles than are needed by the dissymmetry technique. A double extrapolation to both zero concentration *and* zero angle is used to obtain information concerning molecular weight, second-virial coefficient, and chain dimensions, as discussed next.

In the limit of small angles where $P(\theta)$ approaches unity, it can be shown by means of a series expansion of $1/P(\theta)$ that eq. (3.91) becomes^{*}

$$\frac{Kc}{R(\theta)} = \frac{1}{\bar{M}_w} \left[1 + \frac{16}{3} \left(\frac{\pi n}{\lambda} \right)^2 \langle s^2 \rangle \left(\frac{\theta}{2} \right) \right] + 2A_2c. \quad (3.97)$$

* The Rayleigh ratio used in the scattering of dilute polymer solutions is the excess or reduced Rayleigh ratio,

$$\Delta R_\theta = R_\theta(\text{solution}) - R_\theta(\text{solvent}).$$

As illustrated in Figure 3-16, light-scattering data are plotted in the form of $Kc/R(\theta)$ versus $\sin^2(\theta/2) + kc$ for different angles and concentrations (where k is an arbitrary constant added to provide spacing between curves). A double extrapolation to $\theta = 0^\circ$ and $c = 0$, for which the second and third terms on the right of eq. (3.97) become zero, yields \bar{M}_w as the reciprocal of the intercept. As inspection of eq. (3.97) indicates, A_2 is then obtained as one-half of the slope of the extrapolated line at $\theta = 0$; the mean-square radius of gyration is obtained from the initial slope of the extrapolated line at $c = 0$ as

$$\langle s^2 \rangle = \frac{3\bar{M}_w}{16} \left(\frac{\lambda}{\pi n} \right)^2 \times \text{slope (at } c=0 \text{)} . \quad (3.98)$$

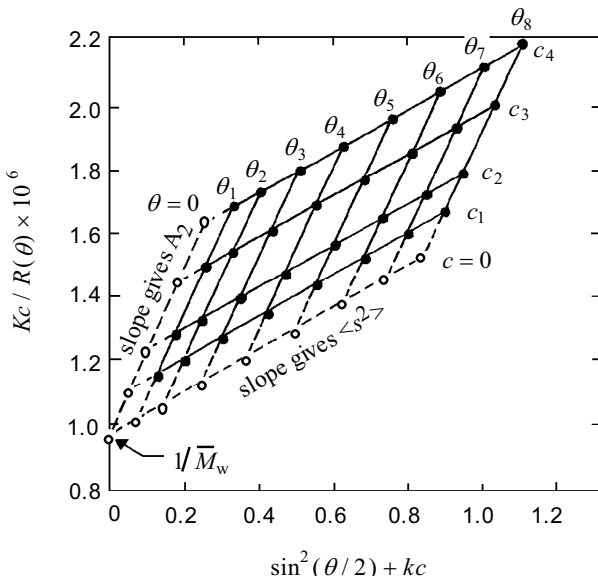


Figure 3-16 Idealized Zimm plot of light-scattering data (\bullet) taken at different angles (θ) and solution concentrations (c). Double extrapolations to zero concentration and zero scattering angle are represented by broken lines.

One obvious difficulty with the Zimm method is that a large number of time-consuming measurements is required; however, the method provides a great deal of information— \bar{M}_w , A_2 , and $\langle s^2 \rangle$. The number of experiments is greatly reduced by using the dissymmetry method; however, chain dimensions are less certain, as discussed next.

Dissymmetry Method. Molecular-weight determination by the *dissymmetry* method requires measurement of the scattered intensity at three angles—typically

45° , 90° , and 135° (see Figure 3-14)—and at several different (dilute) polymer concentrations. A dissymmetry ratio, z , is defined as

$$z = \frac{i(45^\circ)}{i(135^\circ)}. \quad (3.99)$$

Since z is normally concentration-dependent, a value at zero concentration is determined by plotting $(z - 1)^{-1}$ versus concentration. This value can then be used to obtain $P(90^\circ)$ and also $\langle r^2 \rangle^{1/2}$ from published values if the conformational state (e.g., rods, disks, spheres, or random coils) of the polymer in solution is known. In the absence of information to the contrary, a random-coil conformation, typical of flexible-chain polymers, is assumed. Once $P(90^\circ)$ is known, \bar{M}_w can be obtained from the intercept and A_2 obtained from the slope of a plot of $Kc/R(90^\circ)$ versus concentration extrapolated to zero concentration.

Low-Angle Laser Light Scattering (LALLS). In recent years, helium–neon (He–Ne) lasers ($\lambda = 6328 \text{ \AA}$) have replaced conventional light sources in some commercial light-scattering instruments. The high intensity of these light sources permits scattering measurements at much smaller angles (2° to 10°) than is possible with conventional light sources and for smaller samples at lower concentrations. Since at low angles the particle-scattering function, $P(\theta)$, approaches unity, eq. (3.91) reduces to the classical *Debye equation* for scattering by small spherical particles as

$$\boxed{\frac{Kc}{R(\theta)} = \frac{1}{\bar{M}_w} + 2A_2c}. \quad (3.100)$$

Therefore, a plot of $Kc/R(\theta)$ versus c at a single angle gives \bar{M}_w as the inverse of the intercept and A_2 as one-half of the slope.

A representative LALLS plot of $Kc/R(\theta)$ versus c is shown for cellulose acetate (CA) in acetone at 25°C in Figure 3-17. From the intercept, a value of 150,000 is obtained for \bar{M}_w of the CA sample; the second virial coefficient, A_2 , is obtained from the slope as $7.53 \times 10^{-3} \text{ mL mol g}^{-2}$. One limitation of the LALLS method is that chain dimensions cannot be obtained since scattering is measured only at a single angle.

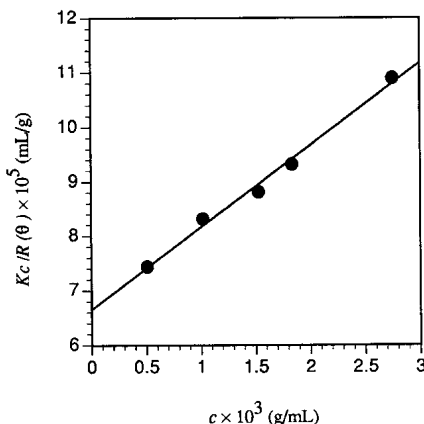


Figure 3-17. Plot of low-angle laser light-scattering data for cellulose acetate in acetone [26].

3.3.3 Intrinsic Viscosity Measurements

A method widely used for routine molecular-weight determination is based upon the determination of the intrinsic viscosity, $[\eta]$, of a polymer in solution through measurements of solution viscosity. Molecular weight is related to $[\eta]$ by the *Mark–Houwink–Sakurada equation* given as

$$[\eta] = K\bar{M}_v^\alpha \quad (3.101)$$

where \bar{M}_v is the viscosity-average molecular weight defined for a discrete distribution of molecular weights (see Section 1.3) as

$$\bar{M}_v = \left[\sum_{i=1}^N N_i M_i^{1+\alpha} / \sum_{i=1}^N N_i M_i \right]^{1/\alpha}. \quad (3.102)$$

Both K and α are empirical (Mark–Houwink) constants that are specific for a given polymer, solvent, and temperature. The exponent α normally lies between the values of 0.5 for a θ solvent and 1.0 for a thermodynamically good solvent. Extensive tables of Mark–Houwink parameters for most commercially important polymers are available [21]. Some typical values for representative polymers are given in Table 3-4. The value of \bar{M}_v normally lies between the values of M_n and M_w obtained by osmometry and light-scattering measurements, respectively. As indicated by eq. (3.102), $\bar{M}_v \equiv \bar{M}_w$ in the case of a thermodynamically good solvent when $\alpha = 1$. The relationship between molecular weights for the *most probable distribution* given by Flory [1] is given by the expression

$$\bar{M}_n : \bar{M}_v : \bar{M}_w :: 1 : \left[(1+a) \Gamma(1+a) \right]^{1/a} : 2$$

where Γ is the gamma function (see Appendix E).

Table 3-4 Mark–Houwink Parameters, K and a , for Some Polymers at 25°C^a

Polymer	Solvent	$K \times 10^3$ (mL g ⁻¹)	a
Cellulose acetate ^b	Tetrahydrofuran	51.3	0.69
Polycarbonate	Tetrahydrofuran	38.9	0.70
Polydimethylsiloxane	Toluene	2.4	0.84
Poly(2,6-dimethyl-1,4-phenylene oxide)	Toluene	28.5	0.68
Poly(methyl methacrylate)	Benzene	5.5	0.76
Polystyrene	Tetrahydrofuran	14	0.70
	Toluene	7.5	0.75
	Benzene	9.2	0.74
Poly(vinyl acetate)	Butanone	42.0	0.62
Poly(vinyl chloride)	Tetrahydrofuran	16.3	0.77

^a Values obtained from light-scattering data.

^b 55.5 wt% acetal content.

Intrinsic viscosity is implicitly expressed by the Huggins equation [27]

$$\boxed{\frac{\eta_i}{c} = [\eta] + k_H [\eta]^2 c} \quad (3.103)$$

where k_H is a dimensionless parameter (the Huggins coefficient) whose value depends upon temperature as well as the specific polymer/solvent combination. The parameter η_i is called the *relative viscosity increment*, which is defined as

$$\eta_i = \frac{\eta - \eta_s}{\eta_s} \quad (3.104)$$

where η and η_s are the viscosities of the dilute polymer solution and pure solvent, respectively. The ratio η/c is commonly called the reduced viscosity, η_{red} , or viscosity number according to recommended IUPAC* nomenclature.

As indicated by the form of eq. (3.103), $[\eta]$ can be obtained from the intercept of a plot of reduced viscosity versus c as shown for cellulose acetate in acetone at 25°C in Figure 3-18. In actual practice, reduced viscosity is obtained at different concentrations not by direct measurement of solution and solvent viscosities but by

* International Union of Pure and Applied Chemistry.

measurement of the time required for a dilute solution (t) and pure solvent (t_s) to fall from one fiducial mark to another in a small glass capillary. If these efflux times are sufficiently long (e.g., >100 s), the relative viscosity increment can be obtained as

$$\eta_i = \frac{t - t_s}{t_s}. \quad (3.105)$$

Efflux times may be noted visually or more precisely by means of commercially available photocell devices.

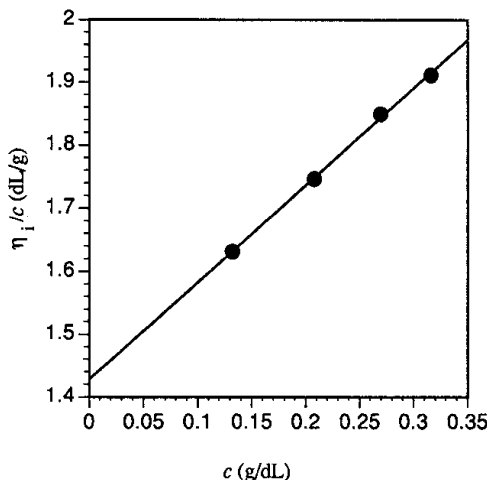


Figure 3-18 Plot of reduced viscosity of a cellulose acetate (intrinsic viscosity of 1.43 dL g^{-1}) in acetone at 25°C [26].

Capillary viscometers may be either Ostwald–Fenske or Ubbelohde types as illustrated in Figure 3-19. The latter have the advantage that different solution concentrations can be made directly in the viscometer by successive dilutions with pure solvent. During measurement, the viscometer is immersed in a constant-temperature bath controlled to within 0.02°C of the set temperature, typically 25° or 30°C .

In addition to determination of molecular weight, measurement of intrinsic viscosity can also be used to estimate chain dimensions in solution. The mean-square end-to-end distance is related to intrinsic viscosity through the relationship [27]

$$\langle r^2 \rangle = \left(\frac{M[\eta]}{\Phi} \right)^{2/3} \quad (3.106)$$

where Φ is considered to be a universal constant ($\Phi \approx 2.1 \pm 0.2 \times 10^{21} \text{ dL mol}^{-1} \text{ cm}^{-3}$) known as the *Flory constant*.

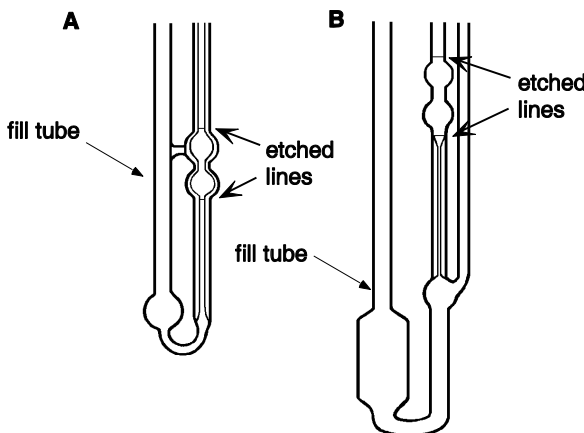


Figure 3-19 Ostwald–Fenske (A) and Ubbelohde (B) capillary viscometers.

3.3.4 Gel-Permeation Chromatography

One of the most widely used methods for the routine determination of molecular weight and molecular-weight distribution is gel-permeation chromatography (GPC), which employs the principle of size-exclusion chromatography (sometimes referred to as SEC) to separate samples of polydisperse polymers into fractions of narrower-molecular-weight distribution. Basic instrumentation for GPC analysis is shown in Figure 3-20. Several small-diameter columns, typically 30 to 50 cm in length, are packed with small, highly porous beads. These are usually fabricated from polystyrene (crosslinked with a small fraction of divinylbenzene as a comonomer) or the packing may be porous glass beads that are usually modified with an ether or diol linkage. Pore diameters of the beads may range from 10 to 10^7 \AA , which approximate the dimensions of polymer molecules in solution. During GPC operation, pure prefiltered solvent is continuously pumped through the columns at a constant flow rate, usually 1 to 2 mL min^{-1} . Then, a small amount (1 to 5 mL) of a dilute polymer solution ($<0.2 \text{ g dL}^{-1}$) is injected by syringe into the solvent stream and carried through the columns. Polymer molecules can then diffuse from this mobile phase into the stationary phase composed of solvent molecules occupying the pore volumes. The smallest polymer molecules are able to penetrate deeply into the interior of the bead pores, but the largest molecules may be completely excluded by the

smaller pores or only partially penetrate the larger ones. As pure solvent elutes the columns after injection, the largest polymer molecules pass through and finally out of the packed columns. These are followed by the next-largest molecules, then the next-largest, and so on, until all the polymer molecules have been eluted out of the column in descending order of molecular weight. Total sample elution in high-resolution columns may require several hours.

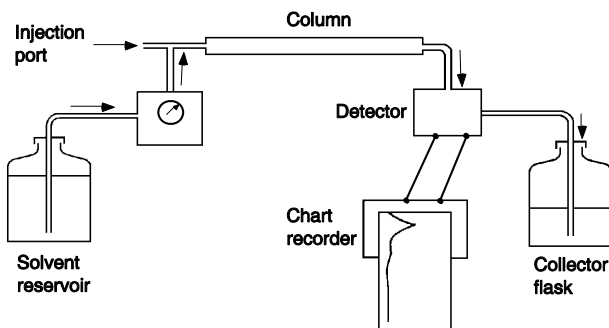


Figure 3-20 Gel-permeation chromatography (GPC). Harry Allcock and Frederick W. Lampe, *Contemporary Polymer Chemistry*. 2nd ed., © 1990, p. 396. Reprinted by permission of Prentice Hall, Englewood Cliffs, NJ.

The concentration of polymer molecules in each eluting fraction can be monitored by means of a polymer-sensitive detector, such as an infrared or ultraviolet device. Usually, the detector is a differential refractometer, which can detect small differences in refractive index between pure solvent and polymer solution. A signal from the detector is recorded as a function of time, which for a fixed flow rate is directly proportional to the elution volume, V_r . A representative GPC chromatogram for a commercial polystyrene sample is shown in Figure 3-21.

For a given polymer, solvent, temperature, pumping rate, and column packing and size, V_r is related to molecular weight. The form of this relation can be found only by comparing elution volumes with those of known molecular weight and narrow-molecular-weight distribution, under identical conditions. Usually, only polymer standards of polystyrene and a few other polymers such as poly(methyl methacrylate) that can be prepared by anionic “living” polymerization (see Section 2.2.2) are available commercially for this purpose. Such standards are available with molecular weights ranging from about 500 to over 2 million with polydispersities as low as 1.06. Since different polymer molecules in the same solvent can have different dimensions, care must be exercised when using polystyrene standards to calibrate elution volumes of other polymers for which standards are not available. The most exact although demanding procedure is to use a universal calibration curve, as illustrated in Figure 3-22.

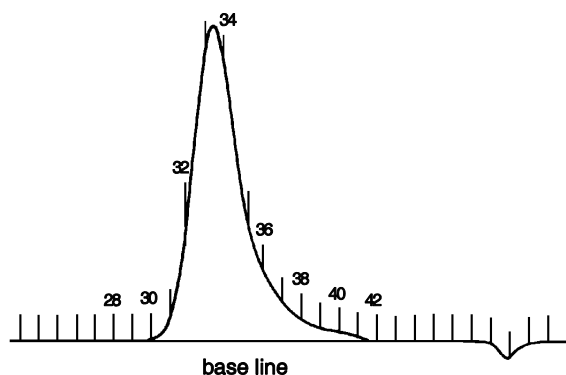


Figure 3-21 GPC chromatogram of polystyrene in tetrahydrofuran at 2.0 mL min^{-1} . Vertical marks represent elution counts. The negative peak at high counts may be due to low-molecular-weight impurities, such as stabilizer, water, or dissolved air. Adapted from L. H. Sperling, *Introduction to Physical Polymer Science*, Fig. 319, p. 88. Copyright © 1986 John Wiley & Sons. Used by permission of John Wiley & Sons, Inc.

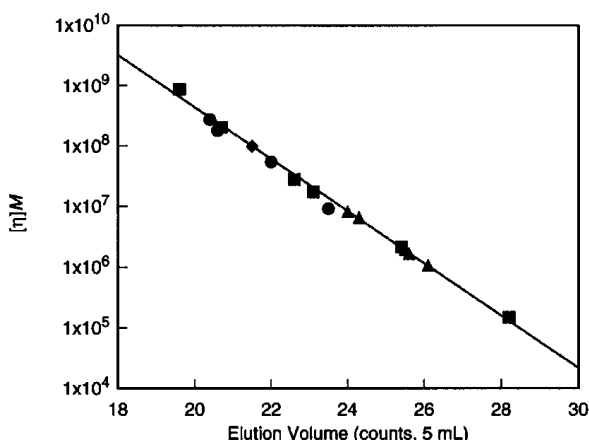


Figure 3-22 Universal GPC calibration curve showing data points for polystyrene (■), poly(vinyl chloride) (▲), polybutadiene (◆), and poly(methyl methacrylate) (●) standards in tetrahydrofuran. Line represents best fit of data [28].

The universal calibration approach is based on the fact that the product $[\eta]M$ is proportional to the hydrodynamic volume of a polymer molecule in solution (see eq (3.106)). This hydrodynamic volume is the effective molecular volume as seen by the pore sites. Universal calibration can be used if the Mark–Houwink constants

(see eq. (3.101)) are known for both the standard and unknown polymer samples in the same solvent and at the same temperature. In the calculation of molecular-weight averages, the signal strength (i.e., peak height in Figure 3-21) is proportional to W_i (eq (1.2)). Once a proper calibration curve is available to relate V_r to the molecular weight (M_i) of the calibration standard, direct calculation of all molecular weights— M_n , M_w , M_z , and even M_{z+1} —is possible, typically by commercially available software. Online coupling of GPC with low-angle light-scattering instrumentation (Section 3.3.2) has enabled rapid online computation of molecular weight without the need for separation calibration of the elution curve.

SUGGESTED READING

- Al-Saigh, Z. Y., *Recent Advances in the Characterization of Polymers and Polymer Blends Using the Inverse Gas Chromatography Method*. Polymer News, 1994. **19**: p. 269.
- Barth, H. G., B. E. Boyes, and C. Jackson, *Size Exclusion Chromatography*. Analytical Chemistry, 1996. **68**: p. 445R.
- Barth, H. G., and J. W. Mays, *Modern Methods of Polymer Characterization*. 1991, New York: John Wiley & Sons.
- Cantow, M. J. R., ed., *Polymer Fractionation*. 1967, New York: Academic Press.
- Danner, R. P., and M. S. High, *Handbook of Polymer Solution Thermodynamics*. 1993, New York: American Institute of Chemical Engineers.
- Einaga, Y., *Thermodynamics of Polymer Solutions and Mixtures*. Progress in Polymer Science, 1994. **19**: p. 1.
- Evans, J., *Gel Permeation Chromatography: A Guide to Data Interpretation*. Polymer Engineering and Science, 1973. **13**: p. 401.
- Forsman, W. C., ed., *Polymers in Solution: Theoretical Considerations and Newer Methods of Characterization*. 1986, New York: Plenum.
- Hansen, C., *Hansen Solubility Parameters: A User's Handbook*. 1999, Boca Raton: CRC Press.
- Hunt, B. J., and S. R. Holding, eds., *Size Exclusion Chromatography*. 1989, New York: Chapman and Hall.
- Morawetz, H., *Macromolecules in Solution*. 1975, New York: John Wiley & Sons.
- Ward, T. C., *Molecular Weight and Molecular Weight Distributions in Synthetic Polymers*. Journal of Chemical Education, 1981. **58**: p. 867.
- Yau, W. W., J. J. Kirkland, and D. D. Bly, *Modern Size-Exclusion Chromatography*. 1979, New York: John Wiley & Sons.

PROBLEMS

- 3.1** Polyisobutylene (PIB) is equilibrated in propane vapor at 35°C. At this temperature, the saturated vapor pressure (p_1^o) of propane is 9050 mm Hg and its density is 0.490 g cm⁻³. Polyisobutylene has a molecular weight of approximately 1 million and a density of 0.915 g

cm^{-3} . The concentration of propane, c , sorbed by PIB at different partial pressures of propane (p_1) is given in the following table. Using this information, determine an average value of the Flory interaction parameter, χ_{12} , for the PIB–propane system.

p_1 (mm Hg)	c (g propane/g PIB)
496	0.0061
941	0.0116
1446	0.0185
1452	0.0183

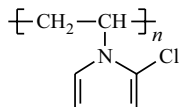
- 3.2** The following osmotic pressure data are available for a polymer in solution:

c (g dL ⁻¹)	h (cm of solvent)
0.32	0.70
0.66	1.82
1.00	3.10
1.40	5.44
1.90	9.30

Given this information and assuming that the temperature is 25°C and that the solvent density is 0.85 g cm⁻³, provide the following:

- (a) A plot of Π/RTc versus concentration, c .
 - (b) The polymer molecular weight and the second virial coefficient, A_2 .
- 3.3** (a) What is the osmotic pressure (units of atm) of a 0.5 wt% solution of poly(methyl methacrylate) ($\bar{M}_n = 100,000$) in acetonitrile (density, 0.7857 g cm⁻³) at 45°C for which $[\eta] = 4.8 \times 10^{-3} \text{ M}^{0.5}$?
- (b) What is the osmotic head in units of cm?
 - (c) Estimate the Flory interaction parameter for polysulfone in methylene chloride.
 - (d) Based upon your answer above, would you expect methylene chloride to be a good or poor solvent for polysulfone?

- 3.4** The osmotic pressure of two samples, A and B, of poly(vinyl pyridinium chloride)



were measured in different solvents. The following data were obtained:

Osmotic Pressure Data in Distilled Water		
Sample	c (g mL ⁻¹)	Π (atm × 10 ³)
A	0.002	29
A	0.005	50
B	0.002	31
B	0.005	52

Osmotic Pressure Data in 0.01 N Aqueous NaCl		
Sample	c (g mL ⁻¹)	Π (atm × 10 ³)
A	0.002	5
A	0.005	13
B	0.002	2
B	0.005	5.5

Discuss these results and account for any features that you consider anomalous.

3.5 The following viscosity data were obtained for solutions of polystyrene (PS) in toluene at 30°C:

c (g dL ⁻¹)	t (s)
0	65.8
0.54	101.2
1.08	144.3
1.62	194.6
2.16	257.0

Using this information:

- (a) Plot the reduced viscosity as a function of concentration.
- (b) Determine the intrinsic viscosity and the value of the Huggins constant, k_H .
- (c) Calculate the molecular weight of PS using Mark–Houwink parameters of $a = 0.725$ and $K = 1.1 \times 10^{-4}$ dL g⁻¹.

3.6 Given that the molecular weight of a polystyrene (PS) repeating unit is 104 and that the carbon–carbon distance is 1.54 Å, calculate the following:

- (a) The mean-square end-to-end distance for a PS molecule of 1 million molecular weight assuming that the molecule behaves as a freely rotating, freely jointed, volumeless chain. Assume that each link is equivalent to a single repeating unit of PS.
- (b) The unperturbed root-mean-square end-to-end distance, $\langle r^2 \rangle_0^{1/2}$, given the relationship for intrinsic viscosity, $[\eta]$, of PS in a θ solvent at 35°C as

$$[\eta] = 8 \times 10^{-4} M^{0.5}$$

where $[\eta]$ is in units of dL g⁻¹.

- (c) The characteristic ratio, C_N , for PS.

3.7 The use of universal calibration curves in GPC is based upon the principle that the product $[\eta]M$, the hydrodynamic volume, is the same for all polymers at equal elution volumes. If the retention volume for a monodisperse polystyrene (PS) sample of 50,000 molecular weight is 100 mL in toluene at 25°C, what is the molecular weight of a fraction of poly(methyl methacrylate) (PMMA) at the same elution volume in toluene at 25°C? The Mark–Houwink parameters, K and a , for PS are given as 7.54×10^{-3} mL g⁻¹ and 0.783, respectively; the corresponding values for PMMA are 8.12×10^{-3} mL g⁻¹ and 0.71.

3.8 Show that the most probable end-to-end distance of a freely jointed polymer chain is given as $(2n\ell^2/3)^{1/2}$.

3.9 The (reduced or excess) Rayleigh ratio (R_θ) of cellulose acetate (CA) in dioxane was determined as a function of concentration by low-angle laser light-scattering measurements. Data are given in the following table. If the refractive index (n_o) of dioxane is 1.4199, the refractive-index increment (dn/dc) for CA in dioxane is 6.297×10^{-2} cm³ g⁻¹, and the wavelength (λ) of the light is 6328 Å, calculate the weight-average molecular weight of CA and the second virial coefficient (A_2).

$c \times 10^3$ (g mL ⁻¹)	$R(\theta) \times 10^5$ (cm ⁻¹)
0.5034	0.239
1.0068	0.440
1.5102	0.606
2.0136	0.790
2.517	0.902

3.10 Chromosorb P was coated with a dilute solution of polystyrene in chloroform, thoroughly dried, and packed into a GC column. The column was then heated in a GC oven and maintained at different temperatures over a range from 200° to 270°C under a helium purge. At each temperature, a small amount of toluene was injected and the time for the solute to elute the column was recorded and compared to that for air. From this information, the specific retention volume was calculated as given in the table below. Using these data, plot the apparent Flory interaction parameter as a function of temperature.

T (°C)	V_g (mL/g-coating)
200	6.55
210	5.58
220	4.66
230	4.07
240	3.38
250	2.87
260	2.88
270	2.38

3.11 (a) Derive eq. (3.72) and then (b) develop an expression that can be used to obtain the exchange interaction parameter, X_{12} , appearing in the Flory equation of state from inverse gas chromatography measurements.

3.12 Derive the expression for osmotic pressure given by eq. (3.83).

3.13 Show how eq. (3.78) for the relation between the Flory–Huggins interaction parameter and the solubility parameters of polymer and solvent was derived.

REFERENCES

1. Flory, P. J., *Principles of Polymer Chemistry*. 1953, Ithaca: Cornell University Press.
2. Flory, P. J., *Statistical Mechanics of Chain Molecules*. 1989, New York: Oxford University Press.
3. Mark, J. E., *Rubber Elasticity*. Journal of Chemical Engineering, 1981. **58**(11): p. 898–903.
4. Wool, R. P., *Polymer Entanglements*. Macromolecules, 1993. **26**: p. 1564–1569.
5. Flory, P. J., *Conformations of Macromolecules in Condensed Phases*. Pure and Applied Chemistry, 1984. **56**(3): p. 305–312.
6. Gee, G., and L. R. G. Treloar, *The Interaction between Rubber and Liquids. I. A Thermodynamical Study of the System Rubber–Benzene*. Transactions of the Faraday Society, 1942. **38**: p. 147–165.
7. Flory, P. J., *Thermodynamics of High Polymer Solutions*. Journal of Chemical Physics, 1941. **9**: p. 660–661.
8. Flory, P. J., *Thermodynamics of High Polymer Solutions*. Journal of Chemical Physics, 1942. **10**: p. 51–61.
9. Huggins, M. L., *Solutions of Long Chain Compounds*. Journal of Chemical Physics, 1941. **9**: p. 440.
10. Huggins, M. L., *Theory of Solutions of High Polymers*. Journal of the American Chemical Society, 1942. **64**: p. 1712–1719.
11. Flory, P. J., *Thermodynamics of Polymer Solutions*. Discussions of the Faraday Society, 1970. **49**: p. 7–29.
12. Flory, P. J., and W. R. Krigbaum, *Statistical Mechanics of Dilute Polymer Solutions. II*. Journal of Chemical Physics, 1950. **18**(8): p. 1086–1094.
13. Koningsveld, R., L. A. Kleintjens, and H. M. Schoffeleers, *Thermodynamic Aspects of Polymer Compatibility*. Pure and Applied Chemistry, 1974. **39**: p. 1–31.
14. Flory, P. J., *Statistical Thermodynamics of Liquid Mixtures*. Journal of the American Chemical Society, 1965. **87**: p. 1833–1838.
15. Sanchez, I. C., and R. H. Lacombe, *Statistical Thermodynamics of Polymer Solutions*. Macromolecules, 1978. **11**: p. 1145–1156.
16. Jain, R. K., and R. Simha, *On the Statistical Thermodynamics of Multicomponent Fluids: Equation of State*. Macromolecules, 1980. **13**: p. 1501–1508.
17. Freeman, P. I., and J. S. Rowlinson, *Lower Critical Points in Polymer Solutions*. Polymer, 1961. **1**: p. 20–26

18. Lipson, J. E. G., and J. E. Guillet, *Study of Structure and Interactions in Polymers by Inverse Gas Chromatography*, in *Developments in Polymer Characterisation*, J. V. Dawkins, ed. 1982, London: Applied Science Publishers, p. 33–74.
19. Everett, D. H., *Effect of Gas Imperfection on G.L.C. Measurements: A Refined Method for Determining Activity Coefficients and Second Virial Coefficients*. Transactions of the Faraday Society, 1965. **61**: p. 1637–1645.
20. Biros, J., L. Zeman, and D. Patterson, *Prediction of the χ Parameter by the Solubility Parameter and Corresponding States Theory*. Macromolecules, 1971. **4**: p. 30–35.
21. Brandrup, J., E. H. Immergut, and E. A. Grulke, eds., *Polymer Handbook*. 4th ed. 1999, New York: John Wiley & Sons.
22. Zoller, P., and D. J. Walsh, *Standard Pressure-Volume-Temperature Data for Polymers*. 1995, Lancaster: Technomic.
23. Scatchard, G., *Equilibria in Non-electrolyte Solutions in Relation to the Vapor Pressures and Densities of the Components*. Chemical Reviews, 1931. **8**: p. 321–333.
24. Hildebrand, J. H., and R. L. Scott, *The Solubility of Non-electrolytes*. 1959, New York: Reinhold.
25. Hansen, C. M., *The Three Dimensional Solubility Parameter—Key to Paint Component Affinities: I. Solvents, Plasticizers, Polymers, and Resins*. Journal of Paint Technology, 1967. **39**: p. 104–117.
26. Wang, C.-S., *The Effect of Solvent Quality on the Viscoelastic Properties of Concentrated Cellulose Acetate Solutions*, PhD Dissertation, Chemical Engineering, University of Cincinnati, 1983.
27. Flory, P. J., and T. G. Fox, *Molecular Configuration and Thermodynamic Parameters from Intrinsic Viscosities*. Journal of Polymer Science, 1950. **5**: p. 745–747.
28. Grubisic, Z., P. Rempp, and H. Benoit, *A Universal Calibration for Gel Permeation Chromatography*. Journal of Polymer Science, Polymer Letters Edition, 1967. **5**: p. 753–759.

This page intentionally left blank